

Status of the solution to the solar neutrino problem based on nonstandard neutrino interactions

S. Bergmann

Department of Particle Physics, Weizmann Institute of Science, Rehovot 76100, Israel

M. M. Guzzo and P. C. de Holanda

Instituto de Física Gleb Wataghin, Universidade Estadual de Campinas, UNICAMP, 13083-970 Campinas SP, Brazil

P. I. Krastev

Department of Physics, University of Wisconsin, Madison, Wisconsin 53706

H. Nunokawa

Instituto de Física Gleb Wataghin, Universidade Estadual de Campinas, UNICAMP, 13083-970 Campinas SP, Brazil

(Received 27 April 2000; published 21 August 2000)

We analyze the current status of the solution to the solar neutrino problem based both on (a) nonstandard flavor-changing neutrino interactions (FCNI) and (b) nonuniversal flavor diagonal neutrino interactions (FDNI). We find that FCNI and FDNI with matter in the Sun as well as in the Earth provide a good fit not only to the total rate measured by all solar neutrino experiments but also to the day-night and seasonal variations of the event rate, as well as the recoil electron energy spectrum measured by the SuperKamiokande Collaboration. This solution does not require massive neutrinos and neutrino mixing in vacuum. Stringent experimental constraints on FCNI from bounds on lepton flavor violating decays and on FDNI from limits on lepton universality violation rule out $\nu_e \rightarrow \nu_\mu$ transitions induced by new physics as a solution to the solar neutrino problem. However, a solution involving $\nu_e \rightarrow \nu_\tau$ transitions is viable and could be tested independently by the upcoming B factories if flavor violating tau decays would be observed at a rate close to the present upper bounds.

PACS number(s): 14.60.Pq, 12.60.-i, 13.15.+g

I. INTRODUCTION

In recent years the accuracy with which the solar neutrino flux is being measured has been improved significantly [1–5]. Better statistics and calibration of the pioneering experiments, as well as the first next-generation experiment at SuperKamiokande, measuring the solar neutrino spectrum and the event rate as a function of the zenith angle with unprecedented precision, have provided a lot of new information about the solar neutrino problem [6]. On the theoretical side, several substantial improvements have been made in the standard solar model (SSM) [7–10] which now includes the diffusion of helium and heavy elements and updated low energy nuclear cross sections relevant to the solar neutrino production [11]. Furthermore, the SSM has received important independent confirmation by the excellent agreement between its predicted sound speeds and recent helioseismological observations [8].

All five solar neutrino experiments [1–5] observe a solar neutrino flux which is smaller than predicted by the SSMs. In order to understand this discrepancy it has been suggested that neutrinos are endowed with properties which are not present in the standard electroweak theory [12]. These new properties allow the electron neutrinos to be converted along their way from the center of the Sun to the detectors on Earth into different neutrino flavors, i.e., into muon, tau, or possibly sterile [13] neutrinos. The fact that the terrestrial experiments are less sensitive to these neutrino flavors explains the observed lower counting rates. The most plausible solution is that neutrinos are massive and there is mixing in the lepton

sector. Then neutrino oscillations in vacuum [14] or matter [15,16] [the Mikheyev-Smirnov-Wolfenstein (MSW) effect] can explain the deficit of observed neutrinos with respect to the predictions of the SSM [17–19].

In his seminal paper, Wolfenstein [15] observed that nonstandard neutrino interactions (NSNI) with matter can also generate neutrino oscillations. In particular this mechanism could be relevant to solar neutrinos interacting with the dense solar matter along their path from the core of the sun to its surface [20–26]. In this case the flavor-changing neutrino interactions (FCNI) are responsible for the off-diagonal elements in the neutrino propagation matrix (similar to the $\Delta m^2 \sin^2 2\theta$ term induced by vacuum mixing). For massless neutrinos, resonantly enhanced conversions can occur due to an interplay between the standard electroweak neutrino interactions and nonuniversal flavor diagonal neutrino interactions (FDNI) with matter [20,27].

While many extensions of the standard model allow for massive neutrinos, it is important to stress that also many new physics models predict new neutrino interactions. The minimal supersymmetric standard model without R parity has been evoked as an explicit model that could provide the FCNI and FDNI needed for this mechanism. Systematic studies of the data demonstrated that resonantly enhanced oscillations induced by FCNI and FDNI for massless neutrinos [21,25], or FCNI in combination with massive neutrinos [21,26] can solve the solar neutrino problem.

In this paper we investigate the current status of the solution to the solar neutrino problem based on NSNI, which is briefly reviewed in Sec. II. In the first part of our study (Sec.

III) we present a comprehensive statistical analysis of this solution. Our analysis comprises both the measured total rates of Homestake [1], GALLEX [2], SAGE [3] and SuperKamiokande [5] and, for the first time in the context of NSNI, the full SuperKamiokande data set (corresponding to 825 effective days of operation), including the recoil electron spectrum and the day-night asymmetry. We have not included in our χ^2 analysis the seasonal variation but we will comment on this effect. For the solar input we take the solar neutrino fluxes and their uncertainties as predicted in the standard solar model by Bahcall and Pinsonneault (BP98 SSM) [9]. The BP98 SSM includes helium and heavy elements diffusion, as well as the new recommended value [11] for the low-energy S -factor, $S_{17} = 19^{+4}_{-2}$ eV b. We also study the dependence of the allowed parameter space on the high energy ^8B neutrino flux, by varying the flux normalization as a free parameter.

In the second part of our study, for the first time a systematic, model-independent investigation of the phenomenological constraints on FCNI and new nonuniversal FDNI relevant for solar neutrinos is presented (Sec. IV). Our two main goals are: (a) to find out whether NSNI can be sufficiently large to provide a viable solution to the solar neutrino problem, and (b) to study various kinds of new interactions in order to single out those new physics models that can provide such interactions. Since the typical energy scales relevant for solar neutrinos are lower than the weak interaction scale and therefore lower than any new physics scale, it is sufficient to discuss the effective operators induced by heavy boson exchange that allow for nonstandard neutrino scattering off quarks or electrons. These operators are related by the $SU(2)_L$ symmetry of the standard electroweak theory to operators that induce anomalous contributions to leptonic decays. Since $SU(2)_L$ violation cannot be large for new physics at or above the weak scale, one can use the upper bounds on lepton flavor violating decays or on lepton universality violation to put model-independent bounds on the relevant nonstandard neutrino interactions.

We find that nonstandard neutrino interactions can provide a good fit to the solar neutrino data if there are rather large nonuniversal FDNI (of order $0.5 G_F$) and small FCNI (of order a few times $10^{-3} G_F$). Our phenomenological analysis indicates that FCNI could only be large enough to provide $\nu_e \rightarrow \nu_\tau$ transitions, while $\nu_e \rightarrow \nu_\mu$ transitions are not relevant for the solution of the solar neutrino problem, because of strong experimental constraints. Large FDNI can only be induced by an intermediate doublet of $SU(2)_L$ (a scalar or a vector boson) or by a neutral vector singlet. We conclude that the minimal supersymmetric model with broken R parity [28] is the favorite model for this scenario.

In Sec. V we discuss how to confirm or exclude the solution to the solar neutrino problem based on nonstandard neutrino interactions by future experiments. We argue that the magnitudes of FCNI parameters necessary for $\nu_e \rightarrow \nu_\tau$ conversion in the sun could be tested independently by the upcoming B -factories. Finally, we discuss briefly the possibility of distinguishing this solution from the others by future solar and long-baseline neutrino oscillation experiments.

II. NEUTRINO FLAVOR CONVERSION INDUCED BY NONSTANDARD NEUTRINO INTERACTIONS

Any model beyond the standard electroweak theory that gives rise to the processes

$$\nu_e f \rightarrow \nu_\ell f, \quad (1)$$

$$\nu_\alpha f \rightarrow \nu_\beta f, \quad (2)$$

where (here and below) $f = u, d, e$ and $\ell = \mu, \tau$ and $\alpha = e, \mu, \tau$, is potentially relevant for neutrino oscillations in the sun, since these processes modify the effective mass of neutrinos propagating in dense matter.

The evolution equations for massless neutrinos that interact with matter via the standard weak interactions and the nonstandard interactions in (1) and (2) are given by [20,21]:

$$i \frac{d}{dr} \begin{pmatrix} A_e(r) \\ A_\ell(r) \end{pmatrix} = \sqrt{2} G_F \begin{pmatrix} n_e(r) & \epsilon_{\nu_\ell}^f n_f(r) \\ \epsilon_{\nu_\ell}^f n_f(r) & \epsilon_{\nu_\ell}^f n_f(r) \end{pmatrix} \begin{pmatrix} A_e(r) \\ A_\ell(r) \end{pmatrix}, \quad (3)$$

where $A_e(r)$ and $A_\ell(r)$ are, respectively, the probability amplitudes to detect a ν_e and ν_ℓ at position r . For neutrinos that have been coherently produced as ν_e in the solar core at position r_0 , the equations in (3) are subject to the boundary conditions $A_e(r_0) = 1$ and $A_\ell(r_0) = 0$. While W -exchange of ν_e with the background electrons gives rise to the well known forward scattering amplitude $\sqrt{2} G_F n_e(r)$, the FCNI in (1) induce a flavor-changing forward scattering amplitude $\sqrt{2} G_F \epsilon_{\nu_\ell}^f n_f(r)$ and the nonuniversal FDNI in (2) are responsible for the flavor diagonal entry $\sqrt{2} G_F \epsilon_{\nu_\ell}^f n_f(r)$ in Eq. (3). Here

$$n_f(r) = \begin{cases} n_n(r) + 2n_p(r), & f = u, \\ 2n_n(r) + n_p(r), & f = d, \end{cases} \quad (4)$$

is the respective fermion number density at position r in terms of the proton (neutron) number density $n_p(r)$ [$n_n(r)$] and

$$\varepsilon = \epsilon_{\nu_\ell}^f \equiv \frac{G_{\nu_\ell \nu_\ell}^f}{G_F} \quad \text{and} \quad \varepsilon' = \epsilon_{\nu_\ell}^f \equiv \frac{G_{\nu_\ell \nu_\ell}^f - G_{\nu_e \nu_e}^f}{G_F}, \quad (5)$$

describe, respectively, the relative strength of the FCNI in (1), and the new flavor diagonal, but nonuniversal interactions in (2). $G_{\nu_\alpha \nu_\beta}^f$ ($\alpha, \beta = e, \mu, \tau$) denotes the effective coupling of the four-fermion operator

$$\mathcal{O}_\nu^f \equiv (\bar{\nu}_\alpha \nu_\beta)(\bar{f} f) \quad (6)$$

that gives rise to such interactions. The Lorentz structure of \mathcal{O}_ν^f depends on the new physics that induces this operator. Operators which involve only left-handed neutrinos (and which conserve total lepton number L) can be decomposed into a $(V-A) \otimes (V-A)$ and a $(V-A) \otimes (V+A)$ component. (Any single new physics contribution that is induced by chiral interactions yields only one of these two components.) It is, however, important to note that only the vector part of the

background fermion current affects the neutrino propagation for an unpolarized medium at rest [15,29]. Hence only the $(V-A) \otimes (V)$ part of \mathcal{O}_ν^f is relevant for neutrino oscillations in normal matter. One mechanism to induce such operators is due to the exchange of heavy bosons that appear in various extensions of the standard model. An alternative mechanism arises when extending the fermionic sector of the standard model and is due to Z -induced flavor-changing neutral currents (FCNCs). For a discussion of Z -induced FCNC effects on solar neutrinos, see Refs. [30,31].

A resonance occurs when the diagonal entries of the evolution matrix in Eq. (3) coincide at some point r_{res} along the trajectory of the neutrino, leading to the resonance condition

$$\epsilon'_{\nu_f} n_f(r_{\text{res}}) = n_e(r_{\text{res}}). \quad (7)$$

An immediate consequence is that new FDNI for $f=e$ alone cannot induce resonant neutrino flavor conversions.

As we will see in Sec. IV only $\nu_e \rightarrow \nu_\tau$ conversions are compatible with the existing phenomenological constraints on ϵ'_{ν_e} and ϵ'_{ν_τ} . We note that in the minimal supersymmetric standard model with broken R -parity [28] the relevant parameters are given by

$$\epsilon'_{\nu_\tau} = \frac{\lambda'_{331} \cdot \lambda'_{131}}{4M_{\tilde{b}}^2 \sqrt{2}G_F}, \quad \text{and} \quad \epsilon'_{\nu_e} = \frac{|\lambda'_{331}|^2 - |\lambda'_{131}|^2}{4M_{\tilde{b}}^2 \sqrt{2}G_F}, \quad (8)$$

in terms of the trilinear couplings λ'_{ijk} and the bottom squark mass $M_{\tilde{b}}$.

The neutrino evolution matrix in Eq. (3) vanishes in vacuum and is negligibly small for the matter densities of the Earth's atmosphere. Therefore the probability of finding an electron neutrino arriving at the detector during day time is easily obtained by evolving the equations in (3) from the neutrino production point to the solar surface. Furthermore, typically there are many oscillations between the neutrino production and detection point and a resonance. Therefore the phase information before and after the resonance is usually lost after integration over the production and detection region and one may use classical survival probabilities. Then at day time we have [21]

$$P_{\nu_e \rightarrow \nu_e}^{\text{day}} = |A_e(r_s)|^2 \simeq \frac{1}{2} + \left(\frac{1}{2} - P_c \right) \cos 2\theta_m^p \cos 2\theta_m^s, \quad (9)$$

where r_s is the solar surface position and in the analytic expression in Eq. (9) we denote by θ_m^p and θ_m^s , respectively, the effective, matter-induced mixing at the neutrino production point and at the solar surface. In terms of the new physics parameters ϵ , ϵ' and the fermion densities the effective mixing is given by [20,21]

$$\tan 2\theta_m = \frac{2\epsilon'_{\nu_f} n_f}{\epsilon'_{\nu_f} n_f - n_e}. \quad (10)$$

Note that $\tan 2\theta_m = 2\epsilon'_{\nu_f}/(\epsilon'_{\nu_f} - 1)$ is constant for $f=e$. P_c is the level crossing probability. The approximate Landau-Zener expression is [20,21]

$$P_c = \exp[-\pi\gamma/2] \quad \text{with} \quad \gamma = 4\sqrt{2}G_F \left| \frac{(\epsilon'_{\nu_f}/\epsilon'_{\nu_f})^2}{\epsilon'_{\nu_f}} \cdot \frac{n_e}{\frac{d}{dx}\left(\frac{n_f}{n_e}\right)} \right|_{\text{res}}. \quad (11)$$

When neutrinos arrive at the detector during the night, a modification of the survival probability has to be introduced since the nonstandard neutrino interactions with the terrestrial matter may regenerate electron neutrinos that have been transformed in the sun. Assuming that the neutrinos reach the Earth as an incoherent mixture of the effective mass-eigenstates ν_1 and ν_2 , the survival probability during night time can be written as [32]

$$P_{\nu_e \rightarrow \nu_e}^{\text{night}} = \frac{P_{\nu_e \rightarrow \nu_e}^{\text{day}} - \sin^2 \theta_m^s + P_{2e}(1 - 2P_{\nu_e \rightarrow \nu_e}^{\text{day}})}{\cos 2\theta_m^s}. \quad (12)$$

Here P_{2e} is the probability of a transition from the state ν_2 to the flavor eigenstate ν_e along the neutrino path in the Earth.

For our analysis we assume a step function profile for the Earth matter density, which has been shown to be a good approximation in other contexts (see, e.g., Ref. [33] for a recent analysis of matter effects for atmospheric neutrinos). Then the Earth matter effects on the neutrino propagation correspond to a parametric resonance and can be calculated analytically [34],

$$P_{2e} = \sin^2 \theta_m^s + W_1^2 \cos 2\theta_m^s + W_1 W_3 \sin 2\theta_m^s, \quad (13)$$

where the parameters W_1 and W_3 contain all the information of the Earth density and are defined in Ref. [34]. (The only difference is that in our case also the off-diagonal element of the neutrino evolution matrix varies when the neutrino propagates through the Earth matter.)

It is this interaction with the terrestrial matter that can produce a day-night variation of the solar neutrino flux and, consequently, a seasonal modulation of the data. (Note that this seasonal variation is of a different nature than the one expected for vacuum oscillations from the change of the baseline due to the eccentricity of the Earth's orbit around the sun.)

III. ANALYSIS OF THE SOLAR NEUTRINO DATA

In this section we present our analysis of the solution to the solar neutrino problem based on neutrino flavor conversions induced by NSNI in matter. Our main goal is to determine the values of ϵ and ϵ' that can explain the experimental observations without modifying the standard solar model predictions.

A. Rates

First we consider the data on the total event rate measured by the chlorine (Cl) experiment [1], the gallium (Ga) detectors GALLEX [2], and SAGE [3] and the water Cherenkov experiment SuperKamiokande (SK) [5]. We compute the allowed regions in parameter space according to the BP98 SSM [9] and compare the results with the regions obtained for an arbitrary normalization f_B of the high energy neutrino ^8B neutrino fluxes.

We use the minimal χ^2 statistical treatment of the data following the analyses of Refs. [35,36]. Our χ^2 -function is defined as follows:

$$\chi_R^2(\varepsilon, \varepsilon', f_B) = \sum_{i,j=1,\dots,4} (R_i^{\text{th}}(\varepsilon, \varepsilon', f_B) - R_i^{\text{obs}}) \times [\sigma_R^2]_{ij}^{-1} (R_j^{\text{th}}(\varepsilon, \varepsilon', f_B) - R_j^{\text{obs}}), \quad (14)$$

where R_i^{th} and R_i^{obs} denote, respectively, the predicted and the measured value for the event rates of the four solar experiments ($i = \text{Cl, GALLEX, SAGE, SK}$). The error matrix σ_R contains both the experimental (systematic and statistical) and the theoretical errors.

In Fig. 1 the allowed regions in the parameter space of ε_ν^d and $\varepsilon_\nu'^d$ for neutrino scattering off d -quarks are shown at 90%, 95% and 99% confidence level (C.L.). In Fig. 1(a), the ^8B flux is fixed by the BP98 SSM prediction ($f_B = 1$). The best fit point of this analysis is found at

$$\varepsilon_\nu^d = 3.2 \times 10^{-3} \quad \text{and} \quad \varepsilon_\nu'^d = 0.61, \quad (15)$$

with $\chi_{\min}^2 = 2.44$ for $4 - 2 = 2$ degrees of freedom (DOF). Allowing an arbitrary ^8B flux normalization, a different best fit point is obtained for $(\varepsilon_\nu^d, \varepsilon_\nu'^d) = (2.2 \times 10^{-2}, 0.59)$ and $f_B = 1.36$ with $\chi_{\min}^2 = 0.91$ for $4 - 3 = 1$ DOF. The result of this analysis is shown in Fig. 1(b). (Effects due to deviations of the hep neutrino flux from the standard solar model prediction are expected to be less significant and we do not consider them in this work.)

In Fig. 2 the allowed regions in the parameter space of ε_ν^u and $\varepsilon_\nu'^u$ for neutrino scattering off u -quarks are shown at 90%, 95% and 99% C.L. In Fig. 2(a), the ^8B flux is fixed by the BP98 SSM prediction. The best fit point of this analysis is found at

$$\varepsilon_\nu^u = 1.32 \times 10^{-3} \quad \text{and} \quad \varepsilon_\nu'^u = 0.43, \quad (16)$$

with $\chi_{\min}^2 = 2.64$ for two DOF. Allowing an arbitrary ^8B flux normalization f_B , a different best fit point is obtained for $(\varepsilon_\nu^u, \varepsilon_\nu'^u) = (5.8 \times 10^{-3}, 0.425)$ and $f_B = 1.34$ with $\chi_{\min}^2 = 0.96$ for one DOF. The result of this analysis is shown in Fig. 2(b).

It is remarkable that the neutrino flavor conversion mechanism based on NSNI provides quite a good fit to the total rates despite the fact that the conversion probabilities (9) and (12) do not depend on the neutrino energy. This is unlike the case of the vacuum and the MSW conversion mechanisms which provide the appropriate energy dependence to yield a good fit. For NSNI the only way to distin-

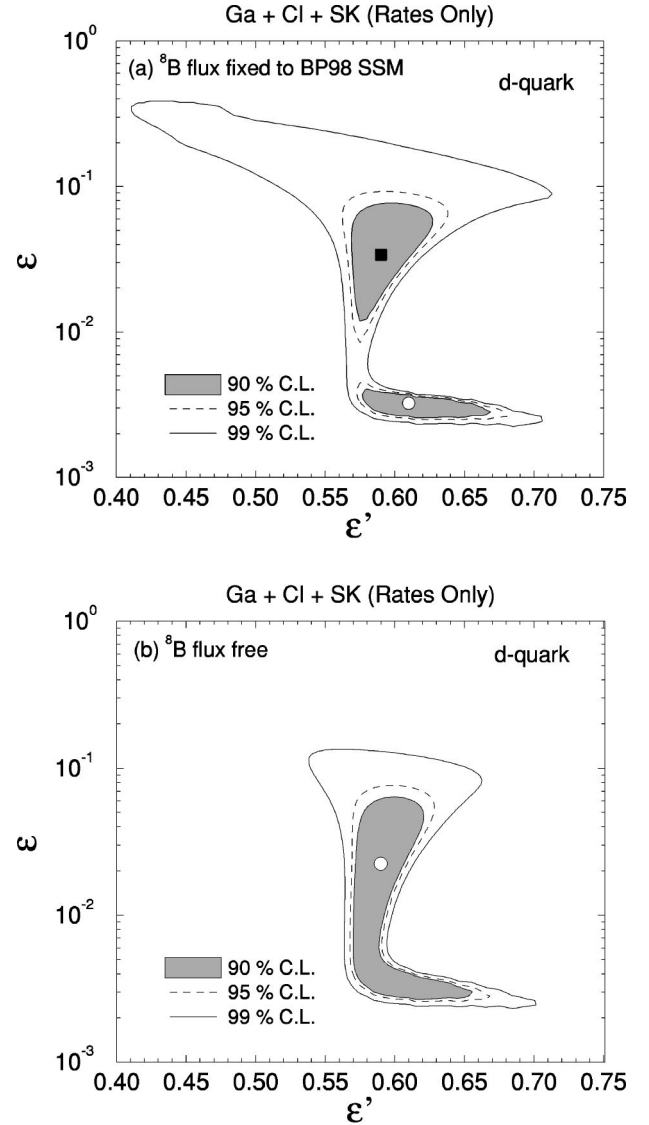


FIG. 1. Region of $\varepsilon = \varepsilon_\nu^d$ and $\varepsilon' = \varepsilon_\nu'^d$ which can explain the total rates measured by the Homestake, GALLEX, SAGE, and SuperKamiokande solar neutrino experiments in terms of nonstandard neutrino interactions with d -quarks. (a) The best fit (indicated by the open circle) is obtained for $(\varepsilon, \varepsilon') = (0.0032, 0.610)$ with $\chi_{\min}^2 = 2.44$ for $4 - 2 = 2$ DOF. A second (local) χ^2 minimum (indicated by the solid square) is found at $(\varepsilon, \varepsilon') = (0.034, 0.610)$ with $\chi^2 = 2.63$. (b) Allowing for an arbitrary ^8B flux normalization f_B , the best fit (indicated by the open circle) is obtained for $(\varepsilon, \varepsilon') = (0.022, 0.590)$ and $f_B = 1.36$ with $\chi_{\min}^2 = 0.91$ for $4 - 3 = 1$ DOF.

guish between neutrinos of different energies is via the position of the resonance r_{res} . Note that according to Eq. (7), r_{res} is a function of ε' only. As can be seen in Fig. 3, n_e/n_f ($f = d, u$) is a smooth and monotonic function of the distance from the solar center r , allowing us to uniquely determine r_{res} for a given value of ε' . From Fig. 3 it follows that a resonance can only occur if $\varepsilon'_d \in [0.50, 0.77]$ for NSNI with d -quarks or $\varepsilon'_u \in [0.40, 0.46]$ for NSNI with u -quarks. For both cases the major part of these intervals corresponds to $r_{\text{res}} \lesssim 0.2 R_\odot$ (R_\odot being the solar radius). For $\varepsilon'_{d,u}$ within the 90% C.L. regions (indicated in Fig. 1 and Fig. 2) we find

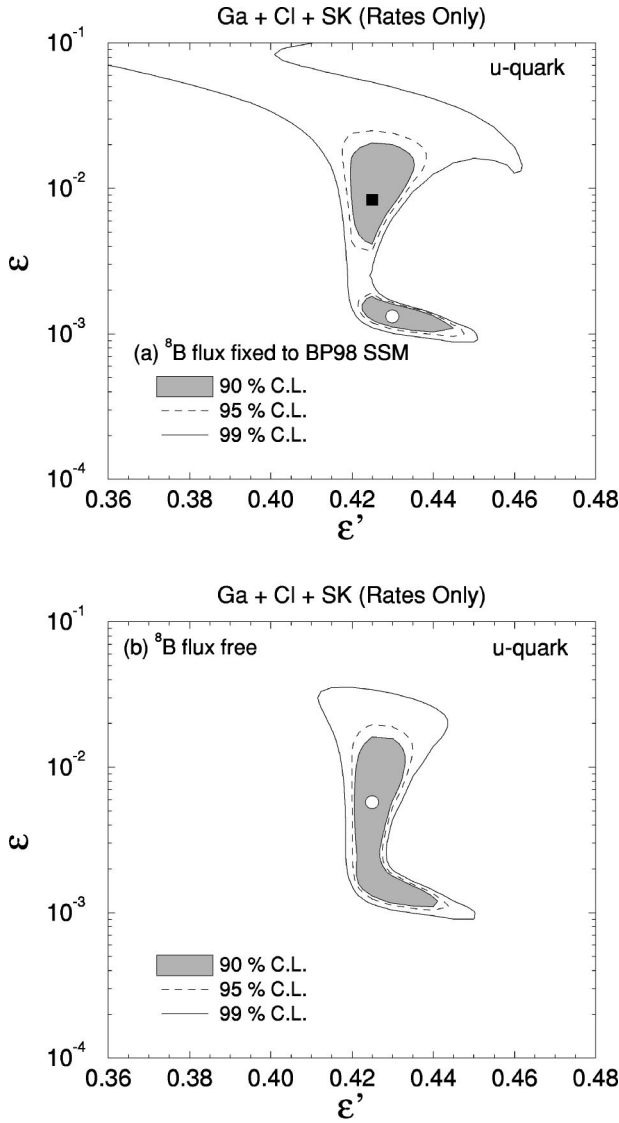


FIG. 2. Same as in Fig. 1 but for u -quarks. (a) The best fit (indicated by the open circle) is obtained for $(\epsilon, \epsilon') = (0.0013, 0.430)$ with $\chi^2_{\min} = 2.75$ for $4 - 2 = 2$ DOF. A second (local) χ^2 minimum (indicated by the solid square) is found at $(\epsilon, \epsilon') = (0.0083, 0.425)$ with $\chi^2 = 2.70$. (b) Allowing for an arbitrary ${}^8\text{B}$ flux normalization f_B , the best fit (indicated by the open circle) is obtained for $(\epsilon, \epsilon') = (0.0058, 0.425)$ and $f_B = 1.34$ with $\chi^2_{\min} = 0.96$ for $4 - 3 = 1$ DOF.

$r_{\text{res}} \approx 0.1 R_{\odot}$. Since the nuclear reactions that produce neutrinos with higher energies in general take place closer to the solar center (see Chap. 6 of Ref. [6] for the various spatial distributions of the neutrino production reactions), a resonance position close to the solar center implies that predominantly the high energy neutrinos are converted by a resonant transition. For $r_{\text{res}} \approx 0.1 R_{\odot}$ practically all ${}^8\text{B}$ neutrinos cross the resonance layer, fewer ${}^7\text{Be}$ neutrinos pass through the resonance, while most of the pp -neutrinos are not be affected by the resonance since their production region extends well beyond the resonance layer. Therefore for most of the allowed region in Figs. 1 and 2 the respective average survival probabilities fulfill

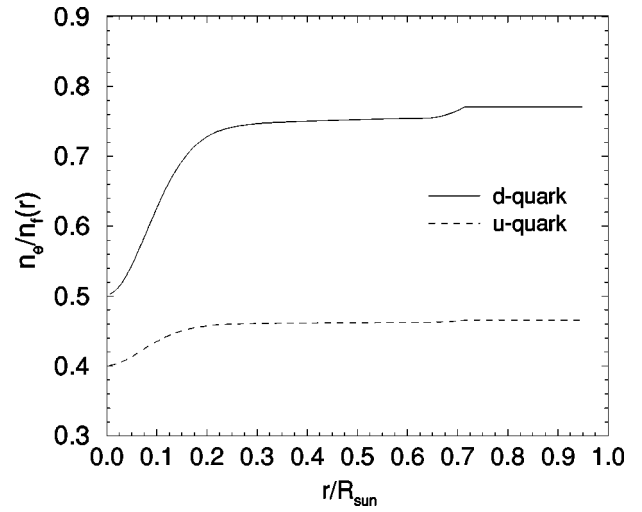


FIG. 3. The ratio of the number density of electron to that of d - and u -quarks in the sun $n_e(r)/n_f(r)$ ($f=d,u$), is plotted as a function of the distance from the solar center.

$$\langle P({}^8\text{B}) \rangle < \langle P({}^7\text{Be}) \rangle < \langle P(pp) \rangle. \quad (17)$$

We note that the above relation is still valid when taking into account that a significant fraction of the pp neutrinos crosses the resonance layer twice, if they are produced just outside resonance. This is—roughly speaking—because a ν_e which undergoes a resonant flavor transition when entering the solar interior at r_{res} is reconverted into a ν_e at the second resonance when it emerges again from the solar core. In our numerical calculations we properly take into account the effects of such double resonances.

An immediate consequence of the relation in Eq. (17) is that as long as $f_B = 1$ the NSNI solution predicts that $R_{\text{SK}} < R_{\text{Cl}} < R_{\text{Ga}}$, which is inconsistent with the observed hierarchy of the rates, $R_{\text{Cl}} < R_{\text{SK}} < R_{\text{Ga}}$, leading to a somewhat worse fit than the standard MSW solutions. However, when treating f_B as a free parameter, for $f_B \sim 1.3 - 1.4$, the SK rate is sufficiently enhanced to give the correct relation between the rates. In this case also the neutral current contribution from $\nu_{\mu, \tau} e^-$ scattering is increased due to a larger $\nu_{\mu, \tau}$ flux, which is consistent with the SuperKamiokande observations. We find that for the best fit points for (ϵ, ϵ') in Figs. 1(b) and 2(b) and $f_B \sim 1.35$, the survival probability for ${}^8\text{B}$, ${}^7\text{Be}$, and pp -neutrinos are ~ 0.24 , 0.4 , and 0.7 , respectively.

In Figs. 1(b) and 2(b) the ${}^8\text{B}$ neutrino flux normalization f_B has been varied as a free parameter in order to study the dependence of the allowed parameter space on the high energy neutrino flux. It is interesting to note that the allowed regions in these figures do not completely contain those in Figs. 1(a) and 2(a), where the boron flux and its uncertainty are determined by the BP98 SSM. In order to explain this apparently inconsistent result we have plotted χ^2 as a function of f_B in Fig. 4, allowing f_B to vary within a sufficiently broad interval ($0 < f_B < 100$) for every point in the (ϵ, ϵ') parameter space. The horizontal lines indicate the 68%, 90%, and 99% C.L. limits for two DOF. The intersection of these lines with the χ^2 curve determines the relevant ranges of the boron flux allowed by the experimental data. The vertical

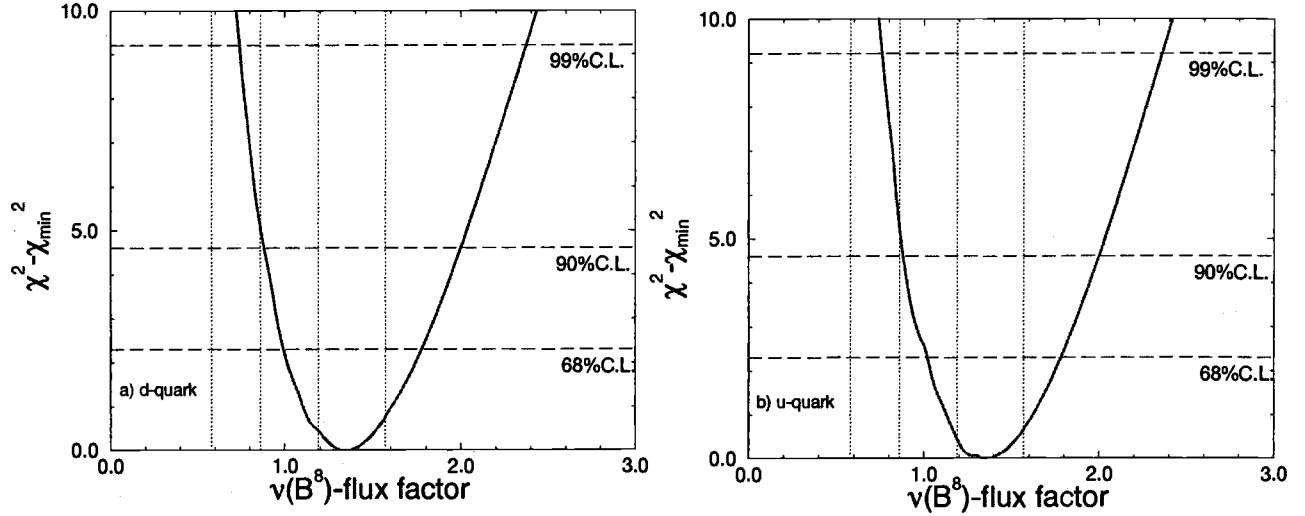


FIG. 4. Minimum χ^2 calculated as a function of the boron neutrino flux for (a) d -quark and (b) u -quark.

dotted lines indicate the 1σ and 3σ ranges of the boron neutrino flux in the BP98 SSM.

Note that the χ^2 minima are obtained for a boron flux significantly larger ($f_B \sim 1.35$) than the one predicted by the SSM ($f_B = 1.0$), as we already anticipated in the discussion of Eq. (17). Moreover, from Fig. 4 it follows that for $f_B < 1$ the fit to the experimental data imposes stronger constraints on the boron flux than the SSM. For $f_B > 1$ the situation is exactly the opposite. Therefore the effect of relaxing f_B from its SSM value is that regions in the $(\varepsilon, \varepsilon')$ parameter space where the averaged survival probability for ${}^8\text{B}$ neutrinos $\langle P({}^8\text{B}) \rangle$ is smaller can be easily compensated by a larger boron flux and obtain a lower value for χ_R^2 . On the other hand, regions where $\langle P({}^8\text{B}) \rangle$ is rather large require a small boron flux which is more difficult to achieve when eliminating the SSM constraint on f_B . This is the main mechanism behind the changes of the allowed regions upon relaxing the SSM constraint on f_B . It explains why the regions with large ε are allowed in Figs. 1(a) and 2(a) and are ruled out in Figs. 1(b) and 2(b). Here $\langle P({}^8\text{B}) \rangle$ is rather large and a small boron flux $f_B \sim 1$ like in the SSM is preferred to explain the data. The opposite occurs in the area between the two disconnected regions in Figs. 1(a) and 2(a). Here $\langle P({}^8\text{B}) \rangle$ is comparatively small and therefore a larger boron flux increases χ_R^2 in this region leading to the merging of the separated contours in Figs. 1(b) and 2(b) when f_B is treated as a free parameter.

B. Zenith angle data

Next, we consider the zenith angle dependence of the solar neutrino data of the SuperKamiokande experiment. As mentioned above, NSNI with matter may affect the neutrino propagation through the Earth, resulting in a difference between the event rates during day and night time. The data obtained by the SuperKamiokande collaboration are divided into five bins containing the events observed at night and one bin for the events collected during the day [37] and have been averaged over the period of SuperKamiokande opera-

tion: 403.2 effective days for the day events and 421.5 effective days for the night events. The experimental results suggest an asymmetry between the total data collected during the day (D) and the total data observed during the night (N) [37]:

$$A = 2 \frac{N - D}{N + D} = 0.065 \pm 0.031(\text{stat}) \pm 0.013(\text{syst}). \quad (18)$$

In order to take into account the Earth matter effect we define the following χ^2 -function that characterizes the deviations of the six measured (Z_i^{obs}) from the predicted (Z_i^{th}) values of the rate as a function of zenith angle:

$$\chi_Z^2(\varepsilon, \varepsilon', \alpha_Z) = \sum_{i=1, \dots, 6} \frac{(\alpha_Z Z_i^{\text{th}}(\varepsilon, \varepsilon') - Z_i^{\text{obs}})^2}{\sigma_{Z,i}^2}. \quad (19)$$

Here $\sigma_{Z,i}$ refers to the total error associated with each zenith angle bin and we have neglected possible correlations between the systematic errors of these bins. Since we are only interested in the shape of the zenith angle distribution, we have introduced an overall normalization factor, α_Z , which is treated as a free parameter and determined from the fit. (Using this procedure also prevents over-counting the data on the total event rate when combining all available data in Sec. III E.) Note that the experimental value of the day-night asymmetry in Eq. (18) is not used in the fit, since the six zenith angle bins already include consistently all the available information about the Earth effects.

In Fig. 5 we show the allowed regions in the $(\varepsilon, \varepsilon')$ parameter space for neutrino scattering off d - and u -quarks, respectively. The contours in Fig. 5 correspond to the allowed regions at 90%, 95%, and 99% C.L. The best fit (indicated by the open circle) is obtained for $(\varepsilon_\nu^d, \varepsilon_\nu'^d) = (0.251, 0.62)$ and $\alpha_Z = 0.819$ with $\chi_{\min}^2 = 1.10$ for neutrino scattering off d -quarks and at $(\varepsilon_\nu^u, \varepsilon_\nu'^u) = (0.229, 0.690)$ and $\alpha_Z = 0.685$ with $\chi_{\min}^2 = 1.44$ for neutrino scattering off u -quarks (having $6 - 3 = 3$ DOF in both cases).

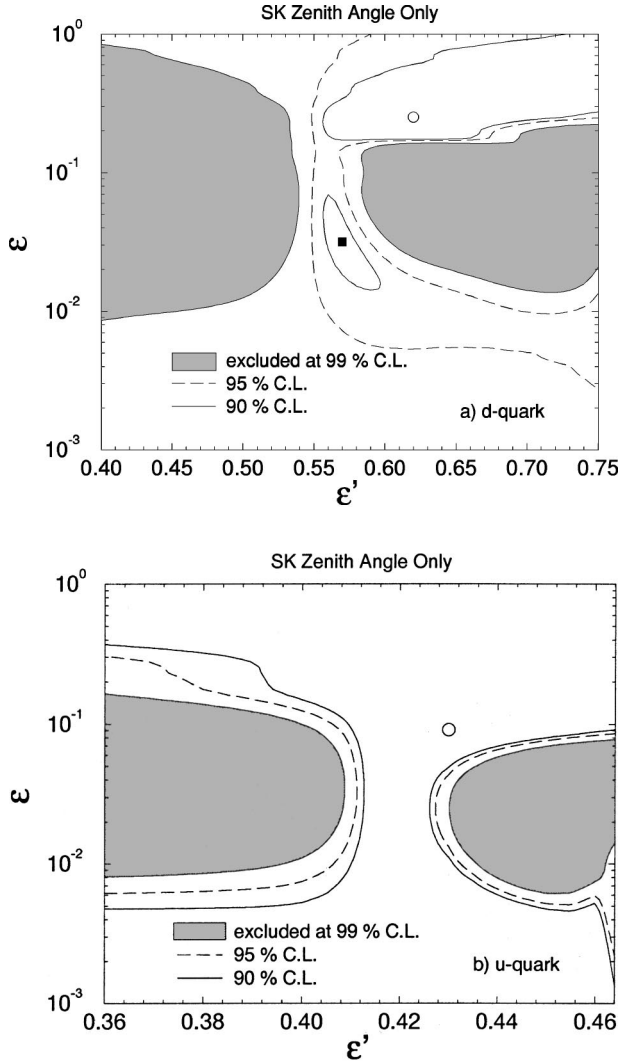


FIG. 5. Region of $\epsilon = \epsilon_\nu^d$ and $\epsilon' = \epsilon_\nu'^d$ which is excluded by day and night data (contained in 1+5 bins) as measured by the SuperKamiokande solar neutrino experiment in terms of nonstandard neutrino interactions with (a) d -quarks and (b) u -quarks. For d -quarks, the best fit (indicated by the open circle) is obtained for $(\epsilon, \epsilon') = (0.251, 0.620)$ and $\alpha_Z = 0.819$ with $\chi^2_{\min} = 1.10$ for $6-3=3$ DOF. A second (local) χ^2 minimum (indicated by the solid square) is found at $(\epsilon, \epsilon') = (0.0316, 0.570)$ and $\alpha_Z = 1.02$ with $\chi^2 = 5.20$. For u -quarks, the best fit (indicated by the open circle) is obtained for $(\epsilon, \epsilon') = (0.229, 0.690)$ and $\alpha_Z = 0.685$ with $\chi^2_{\min} = 1.44$ for $6-3=3$ DOF.

Finally, in Fig. 6 we show the expected zenith angle distributions for SuperKamiokande using the values of (ϵ, ϵ') determined by the best fit. For comparison, we also present in this figure the expected zenith angle distributions for the best fit values of (ϵ, ϵ') found in the combined analysis (that will be discussed in Sec. III E).

C. Recoil electron spectrum

We also consider the measurements of the recoil electron spectrum by SuperKamiokande [37]. The available data, after 825 days of operation, are divided into 18 bins. Seventeen

of these bins have a width of 0.5 MeV and are grouped into two bins for a super low energy analysis with energies between 5.5 and 6.5 MeV and 15 bins with energies ranging from 6.5 MeV (the low energy limit) to 14 MeV. The last bin includes all the events with energies larger than 14 MeV.

Since the electron neutrino survival probability does not depend on the neutrino energy in the NSNI scenario, the spectral distortion of the recoil electrons from ^8B neutrino due to the presence of a $\nu_{\mu, \tau}$ component in the neutrino flux is expected to be very small [38] and therefore, even a relatively small spectral distortion (such as the one expected in small mixing angle MSW solution) could rule out this solution.

The χ^2 -function that characterizes the deviations of the measured (S_i^{obs}) from the predicted (S_i^{th}) values for the electron recoil spectrum therefore provides an important test of the NSNI solution. It is defined as:

$$\chi_S^2(\epsilon, \epsilon', \alpha_S) = \sum_{i,j=1,\dots,18} (\alpha_S S_i^{\text{th}}(\epsilon, \epsilon') - S_i^{\text{obs}}) \times [\sigma_S^2]_{ij}^{-1} (\alpha_S S_j^{\text{th}}(\epsilon, \epsilon') - S_j^{\text{obs}}), \quad (20)$$

where the error matrix (squared)

$$[\sigma_S^2]_{ij} = \delta_{ij} [\sigma_i^2(\text{stat}) + \sigma_i^2(\text{uncorr})] + \sigma_i(\text{corr}) \sigma_j(\text{corr}) + \sigma_i(\text{theor}) \sigma_j(\text{theor}) \quad (21)$$

includes statistical $[\sigma_i(\text{stat})]$ and systematic experimental errors (including both the uncorrelated $[\sigma_i(\text{uncorr})]$ and the correlated $[\sigma_i(\text{corr})]$ contributions) as well as the theoretical errors $[\sigma_i(\text{theor})]$ (see Refs. [17,18] for more details). Again, as in the analysis for the zenith angle dependence, we introduce an overall normalization factor α_S , which is taken as a free parameter and determined from the fit, in order to avoid over-counting the data on the total event rate. Fitting the present data to our scenario we obtain $\chi^2_{\min} = 20.0$ for $18-1=17$ DOF, which is still acceptable at the 27% C.L.

D. Seasonal variations

The Earth matter effects on neutrino flavor transitions induce a seasonal variation of the data (beyond the expected variation of the solar neutrino flux due to the eccentricity of the Earth's orbit) due to the variation of the day and night time during the year. Since these variations can be relevant to other neutrino oscillation scenarios [39], a positive signal could help to distinguish the various solutions and it is worthwhile to analyze the effects of such a variation in the NSNI scenario.

The present SK solar neutrino data do not provide any conclusive evidence in favor of such a variation, but indicate only that the variation seems to be larger for recoil electron energies above 11.5 MeV. In our scenario, however, we do not expect any correlation between the seasonal variation and the recoil electron energies, since the electron neutrino survival probability does not depend on the neutrino energy. Therefore any range of parameters that leads to a considerable seasonal modulation for energies above 11.5 MeV is

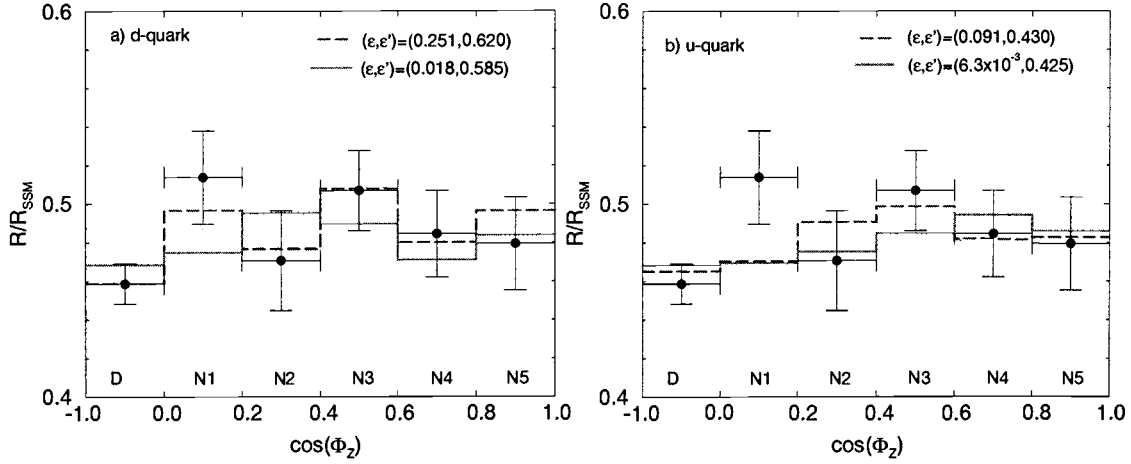


FIG. 6. Expected zenith angle dependence with our best fit values of (ϵ, ϵ') determined only by the SK zenith angle data (dashed line) as well as the combined analysis for (a) d -quarks and (b) u -quarks (full line).

disfavored by the data for lower energies. However, for the range of parameters (ϵ, ϵ') that can solve the solar neutrino problem, Earth regeneration effects are never strong enough to induce a significant seasonal variation. Hence taking into account the data on seasonal variations neither changes the shape of the allowed region, nor the best fit points.

E. Combined analysis

Our final result is the fit derived from the combined analysis of all presently available solar neutrino data. In Figs. 7 and 8 we show the allowed regions for $(\epsilon_\nu^d, \epsilon_\nu'^d)$ and $(\epsilon_\nu^u, \epsilon_\nu'^u)$, respectively, using both the results from the total rates from the chlorine, GALLEX, SAGE, and SuperKamiokande solar neutrino experiments together with the six bins from the SuperKamiokande zenith angle data discussed previously. Although adding the spectral information to our analysis does not change the shape of allowed regions nor the best fit points, it is included in order to determine the quality of the global fit. However, we do not take into account the seasonal variation in our combined χ^2 analysis, since the effect is negligible.

For neutrino scattering off d -quarks, the best fit for the combined data is obtained for

$$\epsilon_\nu^d = 0.028 \quad \text{and} \quad \epsilon_\nu'^d = 0.585, \quad (22)$$

with $\chi_{\min}^2 = 29.05$ for $28 - 4 = 24$ DOF, corresponding to a solution at the 22% C.L. [see Fig. 7(a)]. Allowing $f_B \neq 1$, the best fit is found at $(\epsilon_\nu^d, \epsilon_\nu'^d) = (0.018, 0.585)$ and $f_B = 1.38$ with $\chi_{\min}^2 = 26.62$ for $28 - 5 = 23$ DOF, corresponding to a solution at the 27% C.L. [see Fig. 7(b)]. For neutrino scattering off u -quarks the best fit for the combined data is obtained for

$$\epsilon_\nu^u = 0.0083 \quad \text{and} \quad \epsilon_\nu'^u = 0.425, \quad (23)$$

with $\chi_{\min}^2 = 28.45$ for $28 - 4 = 24$ DOF corresponding to a solution at the 24% C.L. [see Fig. 8(a)]. Allowing $f_B \neq 1$, the best fit is obtained for $(\epsilon_\nu^u, \epsilon_\nu'^u) = (0.0063, 0.426)$ and $f_B = 1.34$ with $\chi_{\min}^2 = 26.59$ for $28 - 5 = 23$ DOF, corresponding

to a solution at the 27% C.L. [see Fig. 8(b)]. These results have to be compared with the fit for standard model neutrinos, that do not oscillate (where the C.L. is smaller than 10^{-7}), as well as to the standard solutions of the solar neutrino problem in terms of usual neutrino oscillations (36% C.L.) [17,18].

Finally, in Fig. 6 we show the expected zenith angle distributions for SuperKamiokande using the best fitted values of (ϵ, ϵ') from the combined analysis.

IV. PHENOMENOLOGICAL CONSTRAINTS ON ϵ AND ϵ'

In this section we investigate whether the allowed regions for the parameters ϵ_ν^f and $\epsilon_\nu'^f$ are at all phenomenologically viable. The analysis of nonstandard neutrino interactions that could be relevant for the solar neutrino problem is similar to the discussions in Refs. [40,41], where the possibility that FCNI explain the LSND results [42,40] or the atmospheric neutrino anomaly [43,41] was discussed.

Generically, extensions of the standard model include additional fields that can induce new interactions: A heavy boson B that couples weakly to some fermion bilinears B_{ij} with the trilinear couplings λ_{ij} , where $i, j = 1, 2, 3$ refer to fermion generations, induces the four-fermion operator $B_{ij}^\dagger B_{kl}$ at tree-level. The effective coupling is given by

$$G_N^{B^\dagger B} = \frac{\lambda_{ij}^* \lambda_{kl}}{4\sqrt{2}M_B^2}, \quad (24)$$

for energies well below the boson mass M_B . Thus, in terms of the trilinear coupling $\lambda_{\alpha f}$ that describes the coupling of some heavy boson B to ν_α ($\alpha = e, \mu, \tau$) and a charged fermion $f = u, d, e$, the effective parameters in (5) are given by

$$\epsilon_{\nu_\ell}^f = \frac{\lambda_{\ell f}^* \lambda_{ef}}{4\sqrt{2}M_B^2 G_F} \quad \text{and} \quad \epsilon_{\nu_\ell}'^f = \frac{|\lambda_{\ell f}|^2 - |\lambda_{ef}|^2}{4\sqrt{2}M_B^2 G_F}. \quad (25)$$

Since any viable extension of the standard model has to contain the SM gauge symmetry, the effective theory ap-

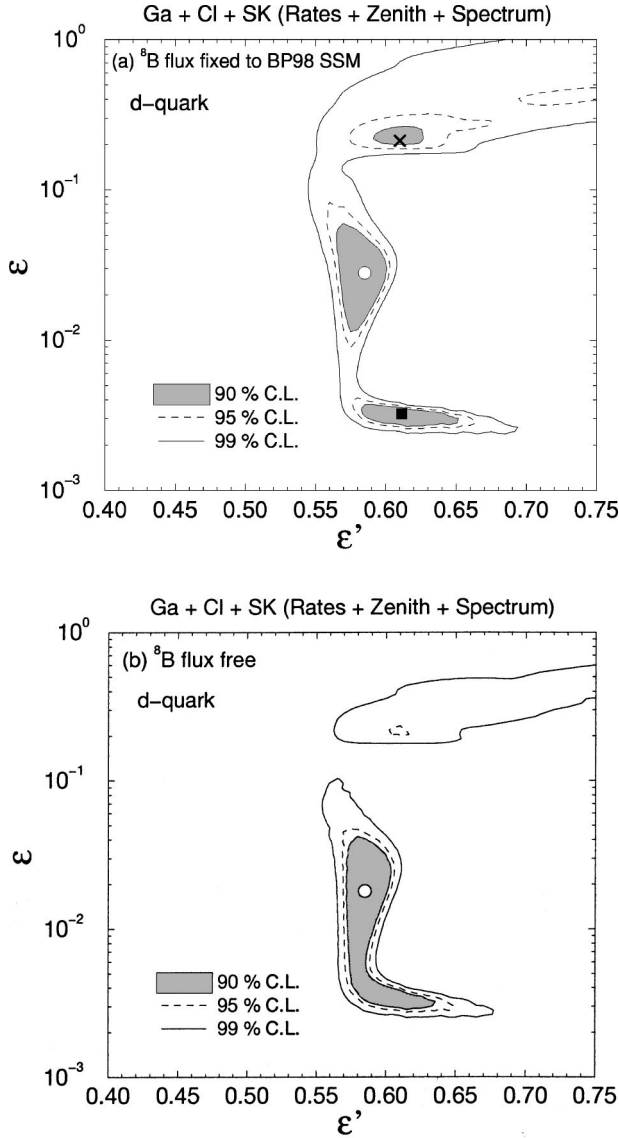


FIG. 7. The allowed region for $\epsilon = \epsilon_\nu^d$ and $\epsilon' = \epsilon_\nu'^d$ obtained by the combined analysis using 4 rates + 6 zenith angle bins + 18 spectrum bins for nonstandard neutrino interactions with d -quarks. (a) Fixing $f_B = 1$ the best fit (indicated by the open circle) is obtained for $(\epsilon, \epsilon') = (0.028, 0.585)$ with $\chi^2_{\min} = 29.05$ for $28 - 4 = 24$ DOF. There are two additional (local) χ^2 minima at $(\epsilon, \epsilon') = (0.0033, 0.610)$ with $\chi^2 = 29.40$ (indicated by the solid square) and $(\epsilon, \epsilon') = (0.21, 0.61)$ with $\chi^2 = 33.1$ (indicated by the cross). (b) Same as in (a) but allowing a free f_B . The best fit (indicated by the open circle) is obtained for $(\epsilon, \epsilon') = (0.018, 0.585)$ and $f_B = 1.38$ with $\chi^2_{\min} = 26.62$ for $28 - 5 = 23$ DOF.

proach presented in Refs. [40,41] is completely sufficient to describe any new physics effect for the energy scales typical to present neutrino oscillation experiments. Even though the effective theory obviously does not contain all the information inherent in the full high-energy theory, the parameters of the effective theory are all of what is accessible at low energies, when the “heavy degrees of freedom” are integrated out.

The crucial point for our analysis is the following: Since the SM neutrinos are components of $SU(2)_L$ doublets, the

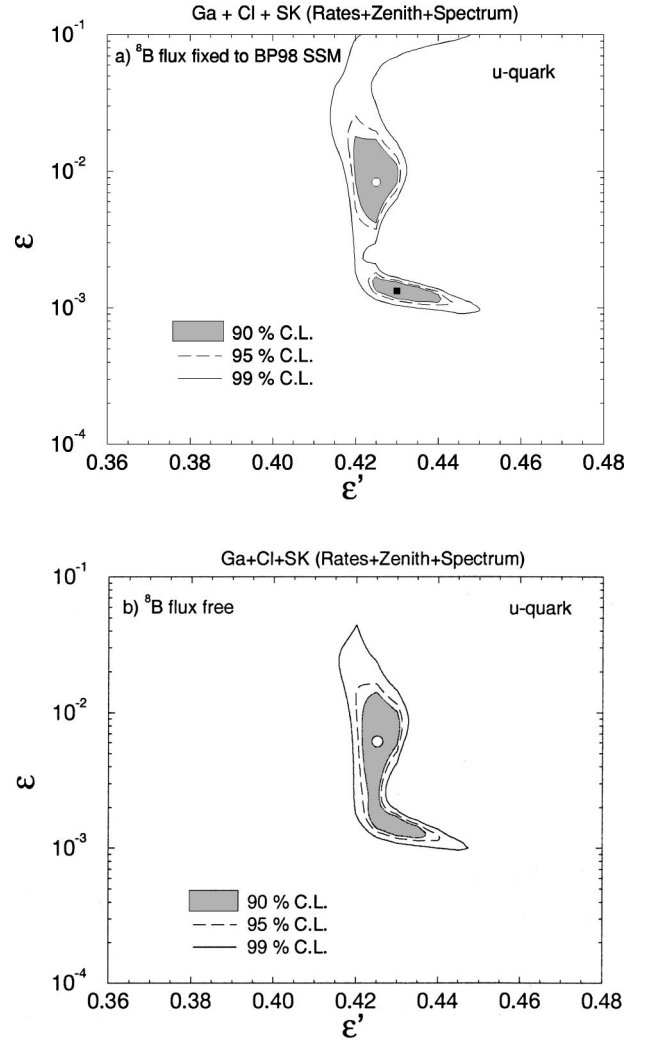


FIG. 8. Same as in Fig. 7 but for u -quarks. (a) Fixing $f_B = 1$ the best fit (indicated by the open circle) is obtained for $(\epsilon, \epsilon') = (0.0083, 0.425)$ with $\chi^2_{\min} = 28.45$ for $28 - 4 = 24$ DOF. A second (local) χ^2 minimum is found at $(\epsilon, \epsilon') = (0.0013, 0.430)$ with $\chi^2 = 30.27$ (indicated by the solid square). (b) Same as in (a) but allowing a free f_B . The best fit (indicated by the open circle) is obtained for $(\epsilon, \epsilon') = (0.0063, 0.426)$ and $f_B = 1.34$ with $\chi^2_{\min} = 26.59$ for $28 - 5 = 23$ DOF.

same trilinear couplings $\lambda_{\alpha f}$ that give rise to nonzero $\epsilon_{\nu/\nu'}^f$ or $\epsilon_{\nu/\nu'}'^f$ also induce other four-fermion operators. These operators involve the $SU(2)_L$ partners of the neutrinos, i.e., the charged leptons, and can be used to constrain the relevant couplings.

Noting that Lorentz invariance implies that any fermionic bilinear B_{ij} can couple to either a scalar (\mathcal{S}) or a vector (\mathcal{V}) boson, it is straightforward to write down all gauge invariant trilinear couplings between the bilinears (that contain SM fermions) and arbitrary bosons \mathcal{S} and \mathcal{V} that might appear in a generic extension of the standard model (see Tables 1–3 of Ref. [41]). From these couplings one then obtains all the effective four-fermion operators relevant to the solution to the solar neutrino problem in terms of NSNI as well as the $SU(2)_L$ -related operators that are used to constrain their ef-

fective couplings. (We do not consider here operators that violate total lepton number which can be induced if there is mixing between the intermediate bosons [44].)

While we refer the reader to Refs. [40,41] for the details of this model-independent approach, we present here two explicit examples relevant to solar neutrinos to demonstrate how $SU(2)_L$ related processes can be used to constrain the parameters $\epsilon_{\nu_\ell}^f$ or $\epsilon_{\nu_\ell}^{f'}$. First, consider the bilinear $\bar{L}f_R$ (where L denotes the lepton doublet and $f=e,u,d$) that couples via a scalar doublet to its hermitian conjugate $\bar{f}_R L$. In terms of the component fields the effective interaction is

$$\begin{aligned} & \frac{\lambda_{\alpha f}^* \lambda_{\beta f}}{M_1^2} (\bar{\nu}_\alpha f_R) (\bar{f}_R \nu_\beta) + \frac{\lambda_{\alpha f}^* \lambda_{\beta f}}{M_2^2} (\bar{l}_\alpha f_R) (\bar{f}_R l_\beta) \\ &= -\frac{\lambda_{\alpha f}^* \lambda_{\beta f}}{2M_1^2} (\bar{\nu}_\alpha \gamma^\mu \nu_\beta) (\bar{f}_R \gamma_\mu f_R) \\ & \quad - \frac{\lambda_{\alpha f}^* \lambda_{\beta f}}{2M_2^2} (\bar{l}_\alpha \gamma^\mu l_\beta) (\bar{f}_R \gamma_\mu f_R), \end{aligned} \quad (26)$$

where $l_\alpha = e_L, \mu_L, \tau_L$ for $\alpha = e, \mu, \tau$. $\lambda_{\alpha f}$ is the trilinear coupling of $\bar{L}_\alpha f_R$ to the scalar doublet and $M_{1,2}$ denote the masses of its $SU(2)_L$ components. The important point is that the scalar doublet exchange not only gives rise to the four-Fermi operator \mathcal{O}_ν^f in (6) [with $(V-A) \otimes (V+A)$ structure], but also produces the $SU(2)_L$ related operator

$$\mathcal{O}_l^f \equiv (\bar{l}_\alpha l_\beta) (\bar{f} f), \quad (27)$$

which has the same Lorentz structure as \mathcal{O}_ν^f , with the neutrinos replaced by their charged lepton partners. Moreover, the effective coupling of \mathcal{O}_l^f , that we denote by $G_{\alpha\beta}^f$, is related to $G_{\nu_\alpha \nu_\beta}^f$ by

$$G_{\nu_\alpha \nu_\beta}^f = G_{\alpha\beta}^f \frac{M_1^2}{M_2^2}. \quad (28)$$

Constructing all the relevant four-fermion operators that are induced by the couplings between the bilinears listed in Tables 1–3 of Ref. [41], one finds that in general \mathcal{O}_l^f is generated together with $\mathcal{O}_{\nu}^{f'}$. Here f' can be different from f only for interactions with quarks, that is in some cases \mathcal{O}_l^u (\mathcal{O}_l^d) is generated together with \mathcal{O}_ν^d (\mathcal{O}_ν^u). The leptonic operator \mathcal{O}_l^e is always generated together with \mathcal{O}_ν^e unless the interaction is mediated by an intermediate scalar $SU(2)_L$ singlet that couples to

$$(L_\ell L_e)_s = \frac{1}{\sqrt{2}} (\bar{\nu}_\ell e_L - \bar{\ell}_L^c \nu_e). \quad (29)$$

Note that the singlet only couples between two different flavors, since the coupling has to be antisymmetric in flavor space. Consequently a singlet that couples to the bilinear $(L_\ell L_e)_s$ cannot induce a nonzero $\epsilon_{\nu_\ell}^e$. The fact that the re-

sulting four-fermion operators only mediate FDNI is true because for the solar neutrinos we only care about $\nu_e \rightarrow \nu_\ell$ transitions. [For atmospheric neutrinos also $\nu_\mu \rightarrow \nu_\tau$ transitions induced by nonstandard neutrino interactions with the electrons are of interest. In this case the coupling of $(L_\mu L_e)_s$ to $(L_\tau L_e)_s^\dagger$ via singlet exchange inducing FCNI is possible [41].]

The effective interactions that are mediated by a scalar singlet of mass M that couples to $(L_\ell L_e)_s$ with the elementary coupling $\lambda_{\ell e}$ are given by

$$\begin{aligned} & \frac{|\lambda_{\ell e}|^2}{M^2} [(\bar{e}_L \nu_\ell^c)(\bar{\nu}_\ell^c e_L) - (\bar{e}_L \nu_\ell^c)(\bar{\ell}_L^c \nu_e) \\ & \quad + (\bar{\nu}_e \ell_L^c)(\bar{\ell}_L^c \nu_e) - (\bar{\nu}_e \ell_L^c)(\bar{\nu}_\ell^c e_L)] \\ &= \frac{|\lambda_{\ell e}|^2}{M^2} [(e_L \gamma^\mu e_L)(\bar{\nu}_\ell \gamma_\mu \nu_\ell) - (e_L \gamma^\mu \nu_e)(\bar{\nu}_\ell \gamma_\mu \ell_L) \\ & \quad + (\bar{\nu}_e \gamma^\mu \nu_e)(\bar{\ell}_L \gamma_\mu \ell_L) - (\bar{\nu}_e \gamma^\mu e_L)(\bar{\ell}_L \gamma_\mu \nu_\ell)], \end{aligned} \quad (30)$$

where we used a Fierz transformation and the identity $\bar{A}^c \gamma^\mu B^c = -\bar{B} \gamma^\mu A$ to obtain (30). One can see that in this case \mathcal{O}_ν^e is generated together with three more operators that have the same effective coupling (up to a sign). However, unlike for the case of intermediate doublets (or triplets), all these operators involve two charged leptons and two neutrinos.

A. Experimental constraints

1. Flavor-changing neutrino interactions

There is no experimental evidence for any nonvanishing $G_{e\ell}^f$. Therefore, whenever \mathcal{O}_l^f is generated together with \mathcal{O}_ν^f , one can use the upper bounds on $G_{e\ell}^f$ to derive constraints on $G_{\nu_e \nu_\ell}^f$. The most stringent constraints on $G_{e\ell}^e$ are due to the upper bounds on $\mu^- \rightarrow e^- e^+ e^-$ and $\tau^- \rightarrow e^- e^+ e^-$ [45,46]:

$$\text{BR}(\mu^- \rightarrow e^- e^+ e^-) < 1.0 \times 10^{-12}, \quad (31)$$

$$\text{BR}(\tau^- \rightarrow e^- e^+ e^-) < 2.9 \times 10^{-6}. \quad (32)$$

Normalizing the above bounds to the measured rates of the related lepton flavor conserving decays, $\text{BR}(\mu^- \rightarrow e^- \bar{\nu}_e \nu_\mu) \approx 100\%$ and $\text{BR}(\tau^- \rightarrow e^- \bar{\nu}_e \nu_\tau) = 0.18$ [46], we obtain

$$\epsilon_\mu^e \equiv G_{e\mu}^e / G_F < 1.0 \times 10^{-6}, \quad (33)$$

$$\epsilon_\tau^e \equiv G_{e\tau}^e / G_F < 4.2 \times 10^{-3}. \quad (34)$$

Note that the bounds on ϵ_ℓ^f do only coincide with those for $\epsilon_{\nu_\ell}^f$ in the $SU(2)$ symmetric limit. We will comment on possible relaxations due to $SU(2)_L$ breaking effects later in Sec. IV B.

To constrain $G_{e\mu}^q$ we use the upper bounds on $\mu \rightarrow e$ conversion from muon scattering off nuclei [46],

$$\frac{\sigma(\mu^- \text{Ti} \rightarrow e^- \text{Ti})}{\sigma(\mu^- \text{Ti} \rightarrow \text{capture})} < 4.3 \times 10^{-12}, \quad (35)$$

$$\frac{\sigma(\mu^- \text{Pb} \rightarrow e^- \text{Pb})}{\sigma(\mu^- \text{Pb} \rightarrow \text{capture})} < 4.6 \times 10^{-11}, \quad (36)$$

$$\frac{\sigma(\mu^- {}^{32}\text{S} \rightarrow e^- {}^{32}\text{S})}{\sigma(\mu^- {}^{32}\text{S} \rightarrow \nu_\mu {}^{32}\text{P}^*)} < 7 \times 10^{-11}, \quad (37)$$

concluding that

$$\epsilon_\mu^q \equiv G_{e\mu}^q / G_F \lesssim 10^{-5} \quad (38)$$

is a conservative upper bound irrespective of the inherent hadronic uncertainties for such an estimate.

To constrain $G_{e\tau}^q$ we may use the upper bounds on various semi-hadronic tau decays that violate lepton flavor [45,46]:

$$\text{BR}(\tau^- \rightarrow e^- \pi^0) < 3.7 \times 10^{-6}, \quad (39)$$

$$\text{BR}(\tau^- \rightarrow e^- \rho^0) < 2.0 \times 10^{-6}, \quad (40)$$

$$\text{BR}(\tau^- \rightarrow e^- \eta) < 8.2 \times 10^{-6}, \quad (41)$$

$$\text{BR}(\tau^- \rightarrow e^- \pi^+ \pi^-) < 1.9 \times 10^{-6}. \quad (42)$$

Let us first consider the tau decays into π^0 and ρ^0 . Since these mesons belong to an isospin triplet we can use the isospin symmetry to normalize the above bounds (39) and (40) by the measured rates of related lepton flavor conserving decays. Using $\text{BR}(\tau^- \rightarrow \nu_\tau \pi^-) = 0.11$ [46] and $\text{BR}(\tau^- \rightarrow \nu_\tau \rho^-) = 0.22$ [47,46], we obtain

$$G_{e\tau}^q(\pi) < 8.2 \times 10^{-3} G_F, \quad \text{and} \quad G_{e\tau}^q(\rho) < 4.2 \times 10^{-3} G_F. \quad (43)$$

Since the π (ρ) is a pseudoscalar (vector) meson its decay probes the axial-vector (vector) part of the quark current.

In general, any semi-hadronic operator \mathcal{O}_I^q can be decomposed into an $I=0$ and an $I=1$ isospin component. Only the effective coupling of the latter can be constrained by the upper bounds on the decays into final states with isovector mesons, like the π and the ρ . If the resulting operator is dominated by the $I=0$ component, the bounds in (43) do not hold. But in this case we can use the upper bound on $\text{BR}(\tau^- \rightarrow e^- \eta)$ in (41). Since the η is an isosinglet, isospin symmetry is of no use for the normalization. However, we can estimate the proper normalization using the relation between the η and π hadronic matrix elements, which is just the ratio of the respective decay constants, $f_\eta/f_\pi \approx 1.3$ [47,46]. Taking into account the phase space effects, we obtain from (41) that

$$G_{e\tau}^q(\eta) < 1.1 \times 10^{-2} G_F. \quad (44)$$

Since the η is a pseudoscalar meson its decay probes the axial-vector part of the $I=0$ component of the quark current, while the neutrino propagation is only affected by the vector part. As we have already mentioned, for any single chiral

new physics contribution the vector and axial-vector parts have the same magnitude and we can use (44) to constrain the isosinglet component of \mathcal{O}_I^q . In case there are several contributions, whose axial-vector parts cancel each other [41], the $I=0$ component could still be constrained by the upper bound on $\text{BR}(\tau^- \rightarrow e^- \pi^+ \pi^-)$ in (42). While the calculation of the rate is uncertain due to our ignorance of the spectra and the decay constants of the isosinglet scalar resonances, we expect that the normalization will be similar to that of the π , ρ , and η discussed before. Finally we note that the decay $\tau^- \rightarrow e^- \omega$ would be ideal to constrain the $I=0$ vector part, but at present no upper bound on its rate is available.

While one can always fine-tune some parameters in order to avoid our bounds, our basic assumption is that this is not the case. Thus from (43) and (44) we conclude that

$$\epsilon_\tau^q \equiv G_{e\tau}^q / G_F \lesssim 10^{-2}. \quad (45)$$

2. Flavor diagonal neutrino interactions

So far we have only discussed the upper bounds on FCNI. However, if the neutrinos are massless then in addition to the FCNI that induce an off-diagonal term in the effective neutrino mass matrix, also nonuniversal flavor diagonal interactions are needed to generate the required splitting between the diagonal terms.

In general any operator that induces such FDNI is related to other lepton flavor conserving operators, that give additional contributions to SM allowed processes, and therefore violate the lepton universality of the SM. Then the upper bounds on lepton universality violation can be used to constrain these operators. Using the relation to the operators that induce the FDNI one may also constrain the latter.

As we mentioned already for massless neutrinos, only a nonzero $\epsilon'_{\nu_\alpha}^q$ ($q=u,d$) can lead to a resonance effect, while FDNI that allow for scattering off electrons alone are insufficient to solve the solar neutrino problem. Therefore we only need to discuss the effective flavor diagonal operator

$$\mathcal{O}_\nu^q \equiv (\bar{\nu}_\alpha \gamma_\mu \nu_\alpha)(\bar{q} \gamma^\mu q), \quad (46)$$

where $\alpha=e,\mu,\tau$ and $q=u_{L,R}, d_{L,R}$.

It is easy to check that for FDNI induced by heavy boson exchange \mathcal{O}_ν^q is always induced together with

$$\mathcal{O}_l^q \equiv (\bar{l}_\alpha \gamma_\mu l_\alpha)(\bar{q}' \gamma^\mu q'), \quad (47)$$

where $q'=u_{L,R}, d_{L,R}$ can be different from q . Moreover, intermediate scalar singlets and triplets (that couple to QL) as well as charged vector singlets and triplets (that couple to $\bar{Q}L$) also give rise to

$$\mathcal{O}_{l\nu}^q \equiv (\bar{l}_\alpha \gamma_\mu \nu_\alpha)(\bar{q}_L \gamma^\mu q'_L), \quad (48)$$

where $q'=u,d$ for $q=d,u$. [See (30) as an example for FDNI mediated by an intermediate scalar singlet.] Since $\mathcal{O}_{l\nu}^q$ induces an additional contribution to the SM weak decay $\tau_L \rightarrow \pi \nu_\tau$ for $\alpha=\tau$ and to $\pi \rightarrow l_\alpha \bar{\nu}_\alpha$ for $\alpha=e,\mu$, the relevant

effective coupling $G_{l\nu}^q$ can be constrained by the upper bounds on lepton universality violation in semi-hadronic decays. The latter leads to a deviation of the parameters

$$R_{e/\mu}^\pi \equiv \sqrt{\frac{1}{N} \frac{\Gamma(\pi^- \rightarrow e^- \bar{\nu}_e)}{\Gamma(\pi^- \rightarrow \mu^- \bar{\nu}_\mu)}} \approx 1 + \frac{G_{e\nu_e}^q - G_{\mu\nu_\mu}^q}{G_F}, \quad (49)$$

$$R_{\tau/\mu}^\pi \equiv \sqrt{\frac{1}{N} \frac{\Gamma(\tau^- \rightarrow \nu_\tau \pi^-)}{\Gamma(\pi^- \rightarrow \mu^- \bar{\nu}_\mu)}} \approx 1 + \frac{G_{\tau\nu_\tau}^q - G_{\mu\nu_\mu}^q}{G_F}, \quad (50)$$

$$R_{\tau/e}^W \equiv \sqrt{\frac{1}{N} \frac{\Gamma(W^- \rightarrow \tau \bar{\nu}_\tau)}{\Gamma(W^- \rightarrow e \bar{\nu}_e)}} \approx 1 + \frac{G_{\tau\nu_\tau}^q - G_{e\nu_e}^q}{G_F}, \quad (51)$$

from unity. Here N denotes a normalization factor, which is just the ratio of the above two rates in the SM such that $R_{\alpha/\beta} = 1$ if $G_{l\alpha\nu_\alpha}^q = G_{l\beta\nu_\beta}^q$. In the approximation we assume that $G_{l\nu}^q \ll G_F$. From the most recent experimental data [48,46] it follows that

$$R_{e/\mu}^\pi = 1.0017 \pm 0.0015, \quad (52)$$

$$R_{\tau/\mu}^\pi = 1.005 \pm 0.005, \quad (53)$$

$$R_{\tau/e}^W = 0.987 \pm 0.023, \quad (54)$$

implying that

$$\epsilon'^q_{\ell} \equiv \frac{G_{\ell\nu_\ell}^f - G_{e\nu_e}^q}{G_F} \lesssim 10^{-2} \quad (55)$$

is a conservative upper bound. If $\mathcal{O}_{l\nu}^q$ is induced together with \mathcal{O}_l^q , then in the $SU(2)_L$ symmetric limit $\epsilon'^q_{\ell} = \epsilon'^q_{\nu}$, but a modest relaxation due to $SU(2)_L$ breaking effects is possible (see Sec. IV B).

It is essential to realize that not all new physics operators that induce the FDNI relevant to solar neutrinos are related to $\mathcal{O}_{l\nu}^q$. For an intermediate $SU(2)_L$ scalar doublet [see Eq. (26) for $f=q$] or a vector doublet (that couples to $\bar{q}^c L$) or a neutral vector singlet, only \mathcal{O}_l^q is induced together with \mathcal{O}_ν^q . In this case one may only use the upper bound on G_{ll}^q that is due to the constraints on compositeness. The present data from $p\bar{p} \rightarrow e^+ e^-, \mu^+ \mu^- + X$ [49,46] imply an upper limit on the scale of compositeness $\Lambda(qq l_\alpha l_\alpha) \gtrsim 1.6$ TeV, which translates into

$$G_{l_\alpha l_\alpha}^q \lesssim 10^{-1} G_F \quad (56)$$

as a conservative estimate for $\alpha=e, \mu$. (One-loop contributions to the Z width due to \mathcal{O}_l^q lead to a similar constraint on G_{ee}^q [50].) However, no upper bound on $\Lambda(qq\tau\tau)$ is available.

For a neutral vector singlet $G_{l_\alpha l_\alpha}^q = G_{\nu_\alpha \nu_\alpha}^q$ and from (5) and (56) it follows that

$$\epsilon'^q_{\nu_\mu} \lesssim 10^{-1}, \quad (57)$$

while there is no model-independent bound on $\epsilon'^q_{\nu_\tau}$. For intermediate $SU(2)_L$ doublets the bound in (57) could be relaxed somewhat, since the effective couplings of the relevant operators may differ due to $SU(2)_L$ breaking effects, which we discuss next.

B. Constraining $SU(2)_L$ breaking effects

The excellent agreement between the SM predictions and the electroweak precision data implies that $SU(2)_L$ breaking effects cannot be large. To show that the upper bounds on G_{ll}^f (or $G_{l\nu}^f$) translate into similar bounds for $G_{\nu\nu}^f$ if their related operators stem from the same $SU(2)_L$ invariant coupling, we recall from Eq. (28) that in general the ratio of the couplings, $G_{\nu_\alpha \nu_\beta}^f / G_{\alpha\beta}^f$ (or $G_{\nu_\alpha \nu_\beta}^f / G_{\alpha\nu_\beta}^f$), is given by ratio M_1^2 / M_2^2 . Here M_1 and M_2 are the masses of the particles belonging to the $SU(2)_L$ multiplet that mediate the processes described by $G_{\alpha\beta}^f$ ($G_{\alpha\nu_\beta}^f$) and $G_{\nu_\alpha \nu_\beta}^f$, respectively. If $M_1 \neq M_2$, this multiplet will contribute to the oblique parameters [51] S, U and, most importantly, T . A fit to the most recent precision data performed in Ref. [41] determined the maximally allowed ratio $(M_1 / M_2)_{\max}^2$ to be at most 6.8 (at 90% C.L.) for intermediate scalars. (Vector bosons in general are expected to have even stronger bounds for the mass ratio). Consequently the upper limits on the effective couplings $G_{\nu\nu}$ agree with those we derived for the corresponding G_{ll}^f (or $G_{l\nu}^f$) within an order of magnitude even for maximal $SU(2)_L$ breaking. Thus, barring fine-tuned cancellations,

$$\epsilon_{\nu_\ell}^f < 6.8 \epsilon_{\ell}^f \quad \text{and} \quad \epsilon'_{\nu_\ell}^f < 6.8 \epsilon'_{\ell}^f, \quad (58)$$

at 90% C.L.

V. IMPLICATIONS FOR FUTURE EXPERIMENTS

In this section we discuss how to test the solution to the solar neutrino problem based on nonstandard neutrino in future neutrino experiments.

Let us consider first the possibility of obtaining stronger constraints on new physics from future laboratory experiments. Our phenomenological analysis shows that FCNI could only be large enough to provide $\nu_e \rightarrow \nu_\tau$ transitions while, model-independently, $\nu_e \rightarrow \nu_\mu$ transitions are irrelevant for solar neutrinos. Even for $\nu_e \rightarrow \nu_\tau$ transitions, the required effective coupling has to be close to its current upper bound, which we derived from limits on anomalous tau decays. Therefore the solution to the solar neutrino problem studied in this paper could be tested by the upcoming B -factories that are expected to improve the present experimental bounds on several rare τ decays. For example, assuming an integrated luminosity of 30 fb^{-1} (corresponding to $3 \times 10^7 \tau$ pairs) for the BaBar [52] experiment, the upper limits on the branching ratios in (39)–(42) could be reduced by one order of magnitude. This would decrease the bound on ϵ_τ^q in (45) to a value close to the smallest possible best fit values for ϵ (cf. Figs. 7 and 8), ruling out a large region of

TABLE I. Future solar neutrino experiments and their rates predicted by the NSNI solution.

Experiment	Start of operation	Main neutrino source	Rate predicted by NSNI
SNO	1999	^8B	0.22–0.43
BOREXINO	2001	^7Be	0.30–0.52
KamLAND	2001	^7Be	0.30–0.52
HELLAZ	>2002	pp	0.52–0.83
HERON	>2000	pp	0.52–0.82

the parameter space and making the NSNI solution increasingly fine-tuned.

Next we consider the implications for future solar neutrino experiments [53–57]. In Table I we present the expected ranges for the event rates (normalized to the SSM expectation in the absence of neutrino flavor transitions) of those experiments, if the solar neutrino problem is explained by NSNI. In Fig. 9 the predicted rates are presented graphically. The ranges correspond to the 95% C.L. regions for $(\varepsilon, \varepsilon')$ in Figs. 7(b) and 8(b). As before we use the BP98 SSM predictions for the initial neutrino fluxes and the survival probability in Eq. (9) to compute the expected rates for each of the five detectors. Specifically, there are three types of detectors: (a) The Sudbury Neutrino Observatory (SNO) [53], which is measuring the ^8B neutrino charged current (CC) rate, (b) the BOREXINO [54] and KamLAND [55] experiments that are designed to observe the ^7Be neutrino signal and (c) the HELLAZ [56] and HERON [57] experiments dedicated to a precise measurement of the low-energy pp neutrino flux.

The predictions for the rates in Table I reflect the relation between the predominant neutrino fluxes that we presented in Eq. (17), i.e., neutrinos with higher energies are in general produced closer to the solar center and therefore more likely to pass through a resonance and undergo flavor conversion.

As can be seen from Fig. 9 the suppression pattern of the NSNI solution is clearly different from the one predicted by the small angle MSW solution (c.f. Fig. 1 of Ref. [58]). But there is a striking similarity between the NSNI solution and the LMA solution, including the preference for large f_B (c.f. Fig. 7 of Ref. [17]), the absence of a ^8B spectral distortion and the modest day-night effect. Consequently, using solar neutrino data, it will be difficult to distinguish the NSNI scenario from the LMA MSW solution. We note, however, that the KamLAND experiment will provide an independent test of the oscillation parameters of the LMA MSW solution by observing antielectron neutrinos from several nuclear reactors around the Kamioka mine in Japan. Thus, if KamLAND would indeed confirm the LMA MSW solution, then the NSNI solution discussed in this paper will be irrelevant.

Since SNO [53] already started taking data and is expected to have some results soon, let us consider some implication for this experiment. As we have pointed out one of the important features of the NSNI conversion mechanism is the absence of any distortion in the solar neutrino spectrum even though the averaged survival probabilities of neutrinos

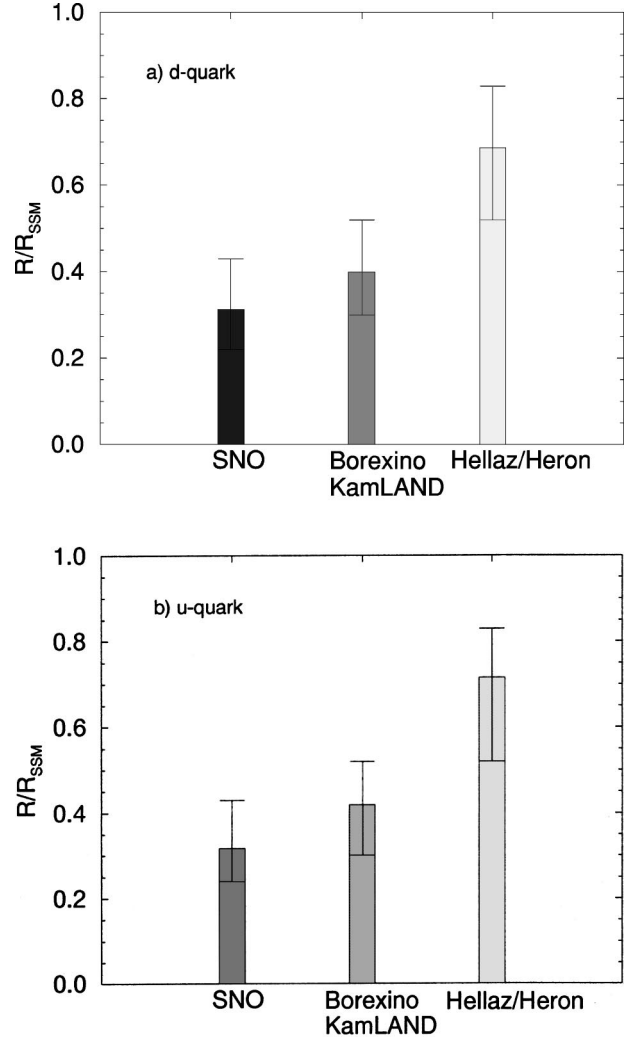


FIG. 9. The predicted ranges of the ratios of event rates for SNO, BOREXINO, and HELLAZ/HERON to the corresponding event rates predicted from the SSM assuming that the neutrino conversion induced by FCNI as well as FDNI is the solution to the solar neutrino problem. Histograms indicate the predictions with the best fitted parameters whereas the error bars indicate the range determined by varying parameters within 95% C.L. regions for $(\varepsilon, \varepsilon')$ in Figs. 7(b) and 8(b).

from different nuclear reactions in the sun are not equal. Due to this feature, the following simple relation between the SuperKamiokande solar neutrino event rate R_{SK} and the SNO CC event rate $R_{\text{SNO}}^{\text{CC}}$ (both normalized by the SSM predictions) holds:

$$R_{\text{SK}} = R_{\text{SNO}}^{\text{CC}}(1 - r) + rf_B, \quad (59)$$

where R_{SK} and $R_{\text{SNO}}^{\text{CC}}$ are defined exactly as in Eqs. (4) and (6) of Ref. [59] and r is given by

$$r \equiv \frac{\int dE_e R(E_e) \int dE_\nu \phi^8(E_\nu) \sigma_{\nu_\mu, \tau e}(E_\nu, E_e)}{\int dE_e R(E_e) \int dE_\nu \phi^8(E_\nu) \sigma_{\nu_e e}(E_\nu, E_e)} \approx \frac{1}{7}. \quad (60)$$

Here, E_e and E_ν are the electron and neutrino energy, respectively, $R(E_e)$ is the SuperKamiokande resolution and efficiency function, ϕ^{8B} is the 8B neutrino flux, and $\sigma_{\nu_e e^-}$ and $\sigma_{\nu_{\mu,\tau} e^-}$ denote the elastic scattering cross sections for $\nu_e e^- \rightarrow \nu_e e^-$ and $\nu_{\mu,\tau} e^- \rightarrow \nu_{\mu,\tau} e^-$, respectively.

We note that R_{SK} and R_{SNO}^{CC} are defined such that $R_{SK} = R_{SNO}^{CC}$ in the absence of neutrino flavor transitions including the case where $f_B \neq 1$. [Strictly speaking, a slight violation of the equality in Eq. (59) could be induced by the Earth matter effect on these two experiments, since they are located at somewhat different latitudes.] Using the relation (59), the true flux of the 8B neutrino flux $(\phi^{8B})_{\text{true}} = f_B(\phi^{8B})_{\text{SSM}}$ could be precisely determined by combining SuperKamiokande and SNO solar neutrino measurements, if the solar neutrino problem is indeed due to NSNI.

Finally let us discuss briefly the possibility of testing the solution studied in this paper by future long-baseline neutrino oscillation experiments. Since only $\nu_e \rightarrow \nu_\tau$ transitions are viable, an independent test would require a ν_τ ($\bar{\nu}_\tau$) appearance experiment using an intense beam of ν_e ($\bar{\nu}_e$), which could be created at future neutrino factories (see, e.g., Ref. [60]).

Assuming a constant density and using the approximation that $n_d \approx n_u \approx 3n_e$ in the Earth, the conversion probability for a neutrino which travels a distance L in the Earth is given by:

$$P(\nu_e \rightarrow \nu_\tau; L) \approx \frac{36\epsilon^2}{36\epsilon^2 + (1 - 3\epsilon')^2} \sin^2 \left[\frac{1}{2} \sqrt{36\epsilon^2 + (1 - 3\epsilon')^2} \sqrt{2} G_F n_e L \right]. \quad (61)$$

Numerically, the oscillation length in the Earth matter can be estimated to be

$$L_{\text{osc}} \approx 8.1 \times 10^3 \left[\frac{2 \text{ mol/cc}}{n_e} \right] \left[\frac{1}{\sqrt{36\epsilon^2 + (1 - 3\epsilon')^2}} \right] \text{ km}. \quad (62)$$

Using Eqs. (61) and (62) and the approximation $n_e \sim 2$ mol/cc (which is valid close to the Earth's surface), we find that, for the case of nonstandard neutrino scattering off d -quark, $P \sim \text{few} \times 10^{-4}$ for K2K ($L = 250$ km) and $P \sim \text{few} \times 10^{-3}$ for MINOS ($L = 732$ km) for our best fit parameters. Similarly for u -quark, $P \sim \text{few} \times 10^{-5}$ for K2K and $P \sim \text{few} \times 10^{-4}$ for MINOS for the best fit parameters. These estimates imply that it would be hard but not impossible, at least for the case of scattering off d -quarks, to obtain some signal of $\nu_e \rightarrow \nu_\tau$ conversions due to NSNI interactions by using an intense ν_e beam which can be created by a muon storage ring [60].

VI. CONCLUSIONS

According to our χ^2 analysis, nonstandard neutrino interactions (NSNI) can provide a good fit to the solar neutrino data provided that there are rather large nonuniversal FDNI (of order $0.5G_F$) and small FCNI (of order $10^{-2} - 10^{-3}G_F$). The fit to the observed total rate, day-night asymmetry, seasonal variation and spectrum distortion of the recoil electron spectrum is comparable in quality to the one for standard neutrino oscillations.

From the model-independent analysis we learn that NSNI induced by the exchange of heavy bosons cannot provide large enough $\nu_e \rightarrow \nu_\mu$ transitions, while $\nu_e - \nu_\tau$ FCNI in principle could be sufficiently strong. However, the current bounds will be improved by the upcoming B -factories, providing an independent test of the NSNI solution. The required large nonuniversal FDNI (for ν_e transitions into both ν_μ and ν_τ) can be ruled out by the upper bounds on lepton universality, unless they are induced by an intermediate doublet of $SU(2)_L$ (a scalar or a vector boson) or by a neutral vector singlet. For $\nu_e \rightarrow \nu_\mu$ there exists a bound due to the limit on compositeness in this case, but for $\nu_e \rightarrow \nu_\tau$ there is no significant constraint at present.

Generically only very few models can fulfill the requirements needed for the solution discussed in this paper: massless neutrinos, small FCNI and relatively large nonuniversal FDNI. As for the vector bosons the most attractive scenario is to evoke an additional $U(1)_{B-3L_\tau}$ gauge symmetry (where B is the baryon number and L_τ denotes the tau lepton number), which would introduce an additional vector singlet that only couples to the third generation leptons and quarks [61]. Among the attractive theories beyond the standard model where neutrinos are naturally massless as a result of a protecting symmetry, are supersymmetric $SU(5)$ models [62] that conserve $B-L$, and theories with an extended gauge structure such as $SU(3)_C \otimes SU(3)_L \otimes U(1)_N$ models [63], where a chiral symmetry prevents the neutrino from getting a mass. These particular models, however, do not contribute significantly to the specific interactions we are interested in this paper. $SU(5)$ models have negligible NSNI since they are mediated by vector bosons which have masses at the GUT scale. $SU(3)_C \otimes SU(3)_L \otimes U(1)_N$ models can provide large ϵ_e and ϵ'_e , but these models do not induce NSNI with quarks. From Eq. (7) it follows that no resonant conversion can occur in this case.

Therefore we conclude that the best candidate for the scenario we studied is supersymmetric models with broken R -parity, where the relevant NSNI are mediated by a scalar doublet, namely the “left-handed” bottom squark. Although in this model neutrino masses are not naturally protected from acquiring a mass, one may either evoke an additional symmetry or assume that nonzero neutrino masses are not in a range that would spoil the solution in terms of the nonstandard neutrino oscillations we have studied in this paper.

Even though we consider the conventional oscillation mechanisms as the most plausible solutions to the solar neutrino problem, it is important to realize that in general new

physics in the neutrino sector include neutrino masses and mixing, as well as new neutrino interactions. While it is difficult to explain the atmospheric neutrino problem [43] and the LSND anomalies [42] by NSNI [40,41], we have shown in this paper that a solution of the solar neutrino problem in terms of NSNI is still viable. The ultimate goal is of course a direct experimental test of this solution. The upcoming solar neutrino experiments will provide a lot of new information which hopefully will reveal the true nature of the solar neutrino problem.

ACKNOWLEDGMENTS

This work was partially supported by Fundação de Amparo à Pesquisa do Estado de São Paulo (FAPESP), Conselho Nacional de Desenvolvimento Científico e Tecnológico (CNPq) and NSF Grant No. PHY-9605140. We thank Y. Grossman, Y. Nir and C. Peña-Garay for helpful discussions. One of us (M.M.G.) would like to thank the Physics Department, University of Wisconsin at Madison, where part of this work was realized, for the hospitality.

-
- [1] Homestake Collaboration, T. B. Cleveland *et al.*, *Astrophys. J.* **496**, 505 (1998).
 - [2] GALLEX Collaboration, W. Hampel *et al.*, *Phys. Lett. B* **447**, 127 (1999).
 - [3] SAGE Collaboration, J. N. Abdurashitov *et al.*, *Phys. Rev. C* **60**, 055801 (1999).
 - [4] Kamiokande Collaboration, Y. Fukuda *et al.*, *Phys. Rev. Lett.* **77**, 1683 (1996).
 - [5] SuperKamiokande Collaboration, Y. Fukuda *et al.*, *Phys. Rev. Lett.* **82**, 1810 (1999).
 - [6] J. N. Bahcall, *Neutrino Astrophysics* (Cambridge University Press, Cambridge, England, 1989).
 - [7] J. N. Bahcall and M. H. Pinsonneault, *Rev. Mod. Phys.* **67**, 781 (1995).
 - [8] J. N. Bahcall, M. H. Pinsonneault, S. Basu, and J. Christensen-Dalsgaard, *Phys. Rev. Lett.* **78**, 171 (1997).
 - [9] J. N. Bahcall, S. Basu, and M. H. Pinsonneault, *Phys. Lett. B* **433**, 1 (1998); see also J. N. Bahcall's home page, <http://www.sns.ias.edu/~jnb>.
 - [10] See also, J. N. Bahcall and R. K. Ulrich, *Rev. Mod. Phys.* **60**, 297 (1988); J. N. Bahcall and M. H. Pinsonneault, *ibid.* **64**, 885 (1992); S. Turck-Chieze *et al.*, *Astrophys. J.* **335**, 415 (1988); S. Turck-Chieze and I. Lopes, *ibid.* **408**, 347 (1993); V. Castellani, S. Degl'Innocenti, and G. Fiorentini, *Astron. Astrophys.* **271**, 601 (1993); V. Castellani *et al.*, *Phys. Lett. B* **324**, 425 (1994).
 - [11] E. G. Adelberger *et al.*, *Rev. Mod. Phys.* **70**, 1265 (1998).
 - [12] For a detailed list of the references on these solutions, see *Frontiers in Physics*, edited by R. Davis, Jr. *et al.* (Addison-Wesley, Reading, MA, 1994), Vol. 92.
 - [13] See, for example, D. O. Caldwell and R. N. Mohapatra, *Phys. Rev. D* **48**, 3259 (1993); J. T. Peltoniemi, D. Tommasini, and J. W. F. Valle, *Phys. Lett. B* **298**, 383 (1993); J. T. Peltoniemi and J. W. F. Valle, *Nucl. Phys.* **B406**, 409 (1993); G. Dvali and Y. Nir, *J. High Energy Phys.* **10**, 014 (1998); G. M. Fuller, J. R. Primack, and Y.-Z. Qian, *Phys. Rev. D* **52**, 1288 (1995); J. J. Gomez-Cadenas and M. C. Gonzalez-Garcia, *Z. Phys. C* **71**, 443 (1996); N. Okada and O. Yasuda, *Int. J. Mod. Phys. A* **12**, 3669 (1997), and references therein.
 - [14] V. N. Gribov and B. M. Pontecorvo, *Phys. Lett.* **28B**, 493 (1969).
 - [15] L. Wolfenstein, *Phys. Rev. D* **17**, 2369 (1978).
 - [16] S. P. Mikheyev and A. Yu. Smirnov, *Sov. J. Nucl. Phys.* **42**, 913 (1985); *Nuovo Cimento C* **9**, 17 (1986).
 - [17] J. N. Bahcall, P. I. Krastev, and A. Yu. Smirnov, *Phys. Rev. D* **58**, 096016 (1998); **60**, 093001 (1999).
 - [18] M. C. Gonzalez-Garcia, P. C. de Holanda, C. Peña-Garay, and J. W. F. Valle, *Nucl. Phys.* **B573**, 3 (2000).
 - [19] G. L. Fogli, E. Lisi, D. Montanino, and A. Palazzo, *Phys. Rev. D* **62**, 013002 (2000).
 - [20] M. M. Guzzo, A. Masiero, and S. T. Petcov, *Phys. Lett. B* **260**, 154 (1991).
 - [21] V. Barger, R. J. N. Phillips, and K. Whisnant, *Phys. Rev. D* **44**, 1629 (1991).
 - [22] E. Roulet, *Phys. Rev. D* **44**, 935 (1991).
 - [23] S. Degl'Innocenti and B. Ricci, *Mod. Phys. Lett. A* **8**, 471 (1993).
 - [24] G. L. Fogli and E. Lisi, *Astropart. Phys.* **2**, 91 (1994).
 - [25] P. I. Krastev and J. N. Bahcall, *hep-ph/9703267*.
 - [26] S. Bergmann, *Nucl. Phys.* **B515**, 363 (1998).
 - [27] Resonant neutrino conversion induced by nonorthogonal massless neutrinos was first discussed by J. W. F. Valle, *Phys. Lett. B* **199**, 432 (1987). However, this mechanism cannot induce a large effect on the solar neutrinos due to the stringent constraints on the model parameters. See also Refs. [30,31].
 - [28] C. S. Aulakh and N. R. Mohapatra, *Phys. Lett.* **119B**, 136 (1983); F. Zwirner, *ibid.* **132B**, 103 (1983); L. J. Hall and M. Suzuki, *Nucl. Phys.* **B231**, 419 (1984); J. Ellis *et al.*, *Phys. Lett.* **150B**, 142 (1985); G. G. Ross and J. W. F. Valle, *ibid.* **151B**, 375 (1985); R. Barbieri and A. Masiero, *Phys. Lett. B* **267**, 679 (1986).
 - [29] S. Bergmann, Y. Grossman, and E. Nardi, *Phys. Rev. D* **60**, 093008 (1999).
 - [30] P. Langacker and D. London, *Phys. Rev. D* **38**, 886 (1988); **38**, 907 (1988); H. Nunokawa, Y.-Z. Qian, A. Rossi, and J. W. F. Valle, *ibid.* **54**, 4356 (1996), and references therein.
 - [31] S. Bergmann and A. Kagan, *Nucl. Phys.* **B538**, 368 (1999).
 - [32] S. P. Mikheyev and A. Yu. Smirnov, *Sov. Phys. Usp.* **30**, 759 (1987).
 - [33] M. Freund and T. Ohlsson, *hep-ph/9909501*.
 - [34] S. T. Petcov, *Phys. Lett. B* **434**, 321 (1998); E. Kh. Akhmedov, *Nucl. Phys.* **B538**, 25 (1999).
 - [35] G. L. Fogli, E. Lisi, and D. Montanino, *Phys. Rev. D* **49**, 3626 (1994).
 - [36] G. L. Fogli and E. Lisi, *Astropart. Phys.* **3**, 185 (1995).
 - [37] Y. Suzuki, "Solar Neutrinos," Lepton Photon Conference, 1999.
 - [38] See J. N. Bahcall, *Neutrino Astrophysics* (Cambridge University Press, Cambridge, England, 1989), Fig. 8.2 for the recoil electron spectra shape from ^8B neutrino due to $\nu_e e^- \rightarrow \nu_e e^-$

- and $\nu_{\mu,\tau}e^- \rightarrow \nu_{\mu,\tau}e^-$ scattering.
- [39] P. C. de Holanda, C. Peña-Garay, M. C. Gonzalez-Garcia, and J. W. F. Valle, Phys. Rev. D **60**, 093010 (1999).
 - [40] S. Bergmann and Y. Grossman, Phys. Rev. D **59**, 093005 (1999).
 - [41] S. Bergmann, Y. Grossman, and D. M. Pierce, Phys. Rev. D **61**, 053005 (2000).
 - [42] LSND Collaboration, C. Athanassopoulos *et al.*, Phys. Rev. Lett. **77**, 3082 (1996); **81**, 1774 (1998).
 - [43] For recent analysis, see, e.g., M. C. Gonzalez-Garcia *et al.*, Phys. Rev. D **58**, 033004 (1998); M. C. Gonzalez-Garcia, H. Nunokawa, O. L. G. Peres, and J. W. F. Valle, Nucl. Phys. **B543**, 3 (1999); N. Fornengo, M. C. Gonzalez-Garcia, and J. W. F. Valle, hep-ph/0002147.
 - [44] S. Bergmann, H. V. Klapdor-Kleingrothaus, and H. Päs, hep-ph/0004048.
 - [45] CLEO Collaboration, W. Bliss *et al.*, Phys. Rev. D **57**, 5903 (1998).
 - [46] Particle Data Group, C. Caso *et al.*, Eur. Phys. J. C **3**, 1 (1998); see also <http://pdg.lbl.gov>.
 - [47] J. F. Donoghue, E. Golowich, and B. R. Holstein, *Dynamics of the Standard Model* (Cambridge University Press, Cambridge, England, 1992).
 - [48] A. Pich, “Review talk at Lepton Photon 99,” Stanford University, 1999, hep-ph/9912294; see also, hep-ph/9711279; hep-ph/9802257.
 - [49] CDF Collaboration, F. Abe *et al.*, Phys. Rev. Lett. **79**, 2198 (1997).
 - [50] M. C. Gonzalez-Garcia, A. Gusso, and S. F. Novaes, J. Phys. G **24**, 2213 (1998).
 - [51] M. E. Peskin and T. Takeuchi, Phys. Rev. Lett. **65**, 964 (1990); Phys. Rev. D **46**, 381 (1992).
 - [52] *The BaBar Physics Book* (SLAC-R-504), Chapter 12.2.6, available at <http://www.slac.stanford.edu/pubs/slacreports/slac-r-504.html>.
 - [53] SNO Collaboration, A. B. McDonald, Nucl. Phys. B (Proc. Suppl.) **77**, 43 (1999).
 - [54] L. Oberauer, Nucl. Phys. B (Proc. Suppl.) **77**, 48 (1999).
 - [55] A. Suzuki, Nucl. Phys. B (Proc. Suppl.) **77**, 171 (1999).
 - [56] HELLAZ Collaboration, A. De Bellefon, Nucl. Phys. B (Proc. Suppl.) **70**, 386 (1999).
 - [57] R. E. Lanou, in *Proceedings of the 8th International Workshop on Neutrino Telescopes*, Venice, Italy, 1999, edited by M. Baldo Ceolin, Vol. I, p. 139.
 - [58] J. N. Bahcall, P. I. Krastev, and A. Yu. Smirnov, hep-ph/0002293.
 - [59] J. N. Bahcall, P. I. Krastev, and A. Yu. Smirnov, Phys. Lett. B **477**, 401 (2000).
 - [60] S. Geer, Phys. Rev. D **57**, 6989 (1998).
 - [61] E. Ma and D. P. Roy, Phys. Rev. D **58**, 095005 (1998); E. Ma, Phys. Lett. B **433**, 74 (1998).
 - [62] L. J. Hall, V. A. Kostelecky, and S. Raby, Nucl. Phys. **B267**, 415 (1986); Y. Okada, hep-ph/9809297.
 - [63] F. Pisano and V. Pleitez, Phys. Rev. D **46**, 410 (1992); P. Frampton, Phys. Rev. Lett. **69**, 2889 (1992).